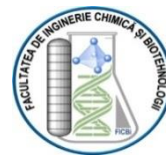




**UNIVERSITATEA "POLITEHNICA" DIN  
BUCUREȘTI  
ȘCOALA DOCTORALĂ - FACULTATEA DE INGINERIE  
CHIMICĂ ȘI BIOTEHNOLOGII**



**Ph.D. THESIS**

**Carbon-based nanomaterials in natural water treatment**

**-Summary-**

**Ph.D. Candidate:**

**Daniela Elisabeta Alexandru (Bogdan)**

**Thesis Supervisor:**

**Prof. eng. dr. Alina Catrinel ION**

**BUCHAREST**

**2023**

## Summary

<b>Abbreviations</b> .....	7
<b>List of figures</b> .....	8
<b>List of tables</b> .....	12
<b>Acknowledgment</b> .....	15
<b>Introduction</b> .....	17
<b>THEORETICAL PART</b> .....	21
<b>Chapter 1. NATURAL WATERS</b> .....	21
1.1. Introduction .....	21
1.2. Classification of natural waters .....	22
1.2.1. Surface waters .....	23
1.2.2. Groundwater .....	23
1.3. Chemical composition of natural waters .....	23
1.3.1. Surface waters .....	23
1.3.2. Groundwater .....	24
1.3.3. Natural mineral waters .....	24
1.4. Quality parameters of natural mineral waters .....	25
1.5. Contaminants present in natural waters .....	27
1.6. Radioactivity of natural waters .....	29
<b>Chapter 2. NATURAL WATER TREATMENT METHODS</b> .....	32
2.1. Classification of treatment methods .....	32
2.2. The application of carbon-based nanomaterials in the treatment of natural waters .....	37
2.3. Carbon-based nanomaterials applied as sorbents in the treatment of natural waters .....	39
2.4. Characterization of sorption processes on carbon-based nanomaterials .....	44
2.4.1. Types of solid-liquid adsorption .....	45
2.4.2. Types of solid-liquid adsorption .....	46
2.4.3. Factors influencing adsorption .....	52
<b>EXPERIMENTAL PART</b> .....	54
<b>Chapter 3. PHYSICAL-CHEMICAL AND RADIOMETRIC CHARACTERIZATION OF SOME NATURAL CARBONATED MINERAL WATERS</b> .....	54
3.1. Introduction .....	54
3.2. Experimental part .....	55
3.2.1. Reagents and instruments .....	55
3.2.2. Collection and preparation of samples .....	56
3.2.3. Instrumentation used in radiometric measurements .....	57
3.3. Results and discussion .....	58
3.3.1. Analysis of the results obtained from the chromatographic determinations .....	58
3.3.2. Results of radiometric analyses .....	67
3.4. Partial conclusions .....	70

<b>Chapter 4. CHROMATOGRAPHIC DETERMINATION OF NITROGEN SPECIES FROM NATURAL MINERAL WATERS BY ION CHROMATOGRAPHY</b> .....	72
4.1. Introduction .....	72
4.2. Experimental part .....	75
4.2.1. Instruments and reagents used for ion separation .....	75
4.2.2. Procedure.....	76
4.2.3. Validation of the optimized analysis method.....	76
4.3. Results and discussion .....	77
4.4. Partial conclusions .....	84
<b>Chapter 5. DISTRIBUTION OF SOME NITROGEN SPECIES DURING WASHING PROCESSES OF NATURAL MINERAL WATER BOTTLING INSTALLATIONS</b> .....	85
5.1. Introduction .....	85
5.2. Experimental part .....	88
5.2.1. The instruments .....	88
5.2.2. Reagents .....	88
5.2.3. Methods of analysis.....	89
5.2.4. Working procedure.....	89
5.3. Results and discussion .....	89
5.4. Partial conclusions .....	97
<b>Chapter 6. AMMONIUM ION ADSORPTION ON UNMODIFIED (PRISTINE) AND OXIDIZED EXFOLIATED GRAPHITE NANO-PLATELETS</b> .....	99
6.1. Introduction .....	99
6.2. Experimental part .....	104
6.2.1. Instruments used.....	104
6.2.2. Reagents .....	105
6.2.3. Working procedure.....	105
Oxidation xGnP.....	105
Description of batch adsorption experiments.....	106
6.3. Results obtained from sorption studies using pristine xGnP as sorbents .....	106
6.3.1. Pristine xGnP characterization .....	106
6.3.2. The effect of contact time .....	107
6.3.3. The effect of temperature variation on the adsorption process .....	107
6.3.4. The effect of the initial concentration of ammonium.....	108
6.3.5. Kinetics of the adsorption process .....	108
6.3.6. Adsorption isotherms of ammonium ions .....	111
6.3.6.1. Langmuir isotherm.....	112
6.3.6.2. Freundlich isotherm .....	113
6.3.6.3. Temkin isotherm.....	114
6.3.6.4. Harkins-Jura and Halsey isotherms .....	115
6.3.7. Thermodynamic study.....	116
6.3.8. Partial conclusions .....	117
6.4. Results of the ammonium ion sorption study on oxidized xGnP.....	118
6.4.1. Characterization ox-xGnP.....	118
6.4.2. Adsorption of $\text{NH}_4^+$ ions on ox-xGnP.....	121
6.4.2.1. The effect of contact time .....	121

---

6.4.2.2. The effect of temperature variation on the adsorption process.....	122
6.4.2.3. The effect of the initial concentration of ammonium .....	122
6.4.2.4. The effect of <i>pH</i> .....	123
6.4.3. Kinetics of the adsorption process .....	123
6.4.4. Adsorption isotherms of ammonium ions .....	125
6.4.4.1. Langmuir isotherm.....	126
6.4.4.2. Freundlich isotherm .....	127
6.4.4.3. Harkins-Jura and Halsey isotherms .....	128
6.4.5. Thermodynamic study.....	131
6.4.6. Partial conclusions.....	133
6.5. Exfoliated carbon nanoplatelets further oxidized as sorbents for ammonium ions .....	134
6.5.1. Introduction.....	134
6.5.2. Experimental part .....	136
6.5.2.1. Materials and methods .....	136
6.5.2.2. Oxidation of xGnP .....	137
6.5.2.3. Adsorption experiments for samples .....	137
6.5.2.4. Methods of analysis .....	138
6.5.3. Results and discussion.....	139
6.5.3.1. Characterization of oxidized xGnP.....	139
6.5.3.1.1. Fourier transform infrared spectra (FTIR).....	139
6.5.3.1.2. Scanning electron microscopy (SEM) .....	140
6.5.3.1.3. Thermogravimetric analysis.....	141
6.5.3.1.4. Titration Boehm .....	142
6.5.4. Results and discussion.....	145
6.5.4.1. Kinetic studies.....	145
6.5.4.2. Study of adsorption isotherms .....	149
6.5.4.3 Thermodynamic analysis .....	153
6.5.4.4. Influence of <i>pH</i> .....	154
6.5.4.5. Influence of other cationic species on sorption .....	155
6.5.4.6. Adsorption mechanism .....	157
6.5.5. Partial conclusions.....	159
<b>Chapter 7. FINAL CONCLUSIONS.....</b>	<b>161</b>
<b>List of published works and participation in conferences.....</b>	<b>164</b>
<b>References .....</b>	<b>166</b>

The doctoral thesis consists of 7 chapters, structured in two parts: the theoretical part, respectively the experimental part.

**The theoretical part** includes a classification of natural waters according to their origin and their chemical and radiochemical composition, followed by the presentation of the legislation in force applied in determining the physical-chemical and radiochemical characteristics of natural and mineral waters. The accepted methods for treating natural mineral waters are then described, taking into account the high degree of purity they must have. It is then presented, taking into account that the treatment of some of these waters allows few methods, variants of carbon-based nanostructured sorbents, possibly to be used, due to the advantages they could offer, both by reducing the amounts of sorbent used in this purpose, as well as by introducing functional groups, which improve their sorption capacity, increasing their selectivity towards certain inorganic species and towards natural radionuclides present in these sources.

**The experimental part of the thesis** includes four chapters.

In the first chapter, characterization studies of natural mineral waters are presented both chemically and radiochemically, depending on the aquifer of origin, presenting a new set of new data regarding the radiochemical composition of mineral waters in Romania. The concentrations of the majority ions highlighted the trends of the chemical evolution depending on the seasonal variations.

Chapter 4 presents an improved method for the analysis of inorganic nitrogen species in aqueous matrices. The purpose of the applied method was to analyze the  $\text{NO}_3^-$  and  $\text{NO}_2^-$  anions present at low concentrations in mineral waters, as well as the concentration of  $\text{NH}_4^+$  ions.

In chapter 5, some influences of the traces of washing agents used in the bottling plants of natural mineral waters were highlighted in changing the concentration ratio of nitrogen species present in these matrices. Natural mineral water matrices contain in their composition  $\text{Fe}^{2+}$  and  $\text{Mn}^{2+}$  cations which, in the presence of oxidizing agents, can naturally generate Fenton-type reactions, in the absence of additional chemical reagents used in these water treatment processes. Under these conditions, the chemical oxidation of the ammonium ions present in the matrix also takes place, thus producing an interconversion of the species with nitrogen and changing the concentrations of nitrate and nitrite ions. One of the purposes of this paper is to study the impact of some natural water treatment methods, taking into account their chemical and radiochemical composition.

The last chapter of the experimental part aimed to study the adsorption process of ammonium ions on carbon-based nanomaterials, by using, as a sorbent, exfoliated graphite nanoplatelets (xGnP) oxidized with  $\text{HNO}_3$  with a reflux time of three hours. xGnPs were chosen due to their irregularly shaped sheets with micrometer-sized dimensions and nanometric thicknesses, less than 100 nm. They provide oxidation centers for obtaining oxidized graphite nanoplatelets (ox-xGnP).  $\text{HNO}_3$  was preferred because it involves a single-step oxidation process with variable oxidation times. An adsorption study was done by controlling the  $\text{pH}$  of the solution and repeatedly washing the sorbents. It is necessary to discriminate between acidic functional groups obtained by different reflux times using the same oxidizing reagent ( $\text{HNO}_3$ ) because it can be assumed that acidic functional groups control the ion exchange process of ammonium ions on carbon nanosorbents in aqueous media, the process being reversible and electrostatic in nature. This method provides a simpler approach to modifying xGnP.

A special attention is given in this paper to the ammonium ion, both as an indicator of the purity of some types of underground waters, and as a pollutant present in natural surface waters. The studies in this work had in mind the removal of this chemical species from the studied aqueous matrices because in natural waters ammonium ions can generate, under favorable conditions, other

species with nitrogen: nitrate and nitrite. The studied sorbents were used to remove ammonium ions from natural and mineral waters, taking into account that they can only be treated with certain exceptions, namely processes that do not have the effect of changing the composition of the water in terms of the characteristic constituents that give it its properties, and the new materials studied in this thesis could fall into these exceptions.

At the end of the doctoral thesis, further research perspectives on the use of carbon-based nanomaterials for the decontamination of natural waters are presented.

## EXPERIMENTAL PART

### **Chapter 3. Physical-chemical and radiometric characterization of some natural carbonated mineral waters**

Natural mineral waters are microbiologically pure natural waters, with a variable content of salts, other mineral substances and radioactive nuclides. In Europe there are more than 1000 recognized brands of water and a much larger number of non-captured mineral water sources.<sup>1</sup>

The European Community requires, through legislation, the fulfillment of certain physical and chemical properties for these natural waters, which, in general, differ from drinking waters.<sup>2,3,4</sup>

The mineral waters in this study come from carbonated water sources, located in the Bucovina region, the samples being collected regularly over two years. The analyzed samples allowed the correlation of the chemical composition of the collected water depending on the seasonal variations and the geochemistry of the aquifer.

An attempt was made to estimate the activity concentration levels of the natural radionuclides present in the water composition and to determine the radiation doses corresponding to them, presenting data for:  $^{238}\text{U}$ ,  $^{232}\text{Th}$ ,  $^{226}\text{Ra}$  și  $^{40}\text{K}$ . Based on the obtained data, both the effective annual doses from these radionuclides were estimated, as well as the total activities  $\alpha$  and  $\beta$  from the samples taken, which according to WHO regulations (World Health Organization) must be lower than  $0,5 \text{ Bq}\cdot\text{L}^{-1}$  for gross-  $\alpha$  and  $1 \text{ Bq}\cdot\text{L}^{-1}$  for gross-  $\beta$ , in natural drinking waters.

#### **Analysis methods:**

- *Chromatographic method used for the determination of ionic species:*
  - the standard chromatographic separation method for anions, SR EN ISO 10304-1:2009 and the standard chromatographic separation method for cations, SR EN ISO 14911:2006.<sup>5</sup>
  - *Measurements by radiometric spectrometry of isotopes with system PROTEAN ORTEC MPC-2000-DP*

#### **Stages in the analysis of the water samples taken:**

- the *pH* and electrical conductivities were measured based on the standards (EN 27888:1993-11) and (DIN 38404-5:1984-01, C5).
- measuring the concentration of  $\text{HCO}_3^-$  ions immediately after opening the vials.
- chromatographic analysis, using standardized analysis methods.
- the concentration of fluoride ions was measured with ion-selective electrodes, based on a previously developed method<sup>6</sup>.

### **3.3. Results and discussion**

#### **3.3.1. Analysis of the results obtained from the chromatographic determinations**

For the analyzed water samples, the concentrations of some anions and cations predominantly present in them were determined ( $\text{Ca}^{2+}$ ,  $\text{Mg}^{2+}$ ,  $\text{Na}^+$ ,  $\text{K}^+$ ,  $\text{NH}_4^+$ ,  $\text{HCO}_3^-$ ,  $\text{SO}_4^{2-}$ ,  $\text{Cl}^-$ ,  $\text{F}^-$ ,  $\text{NO}_3^-$ ),  $\text{O}_2$  dissolved, dry residue), electrical conductivity and *pH*, the data obtained leading to obtaining the characteristic fingerprint of the local geology and the position of the aquifer.

The studied natural water presents, for all 30 selected samples, a high mineralization indicated by the electrical conductivity values, between  $1567$  and  $1883 \mu\text{S}\cdot\text{cm}^{-1}$  (Table 7). Its higher values were recorded at the end of summer, due to the higher temperatures and the lower level of precipitation in this period compared to those in winter and spring. The waters studied, slightly acidic *pH* values, between  $5,87$  and  $6,23$ , slightly lower values being recorded during autumn. The

determined ion concentrations together with the statistical analysis of the monitored data are presented in the Tables 7 and 8.

**Table 7. Chemical composition of the studied natural water: average *pH* values, the electrical conductivity and the average values of the concentrations of the main ions present in water, determined periodically for 36 months**

Proba	<i>pH</i>	C.e. $\mu\text{S}\cdot\text{cm}^{-1}$	$\text{Cl}^{-}$ $\text{mg}\cdot\text{L}^{-1}$	$\text{SO}_4^{2-}$ $\text{mg}\cdot\text{L}^{-1}$	$\text{HCO}_3^{-}$ $\text{mg}\cdot\text{L}^{-1}$	$\text{Na}^{+}$ $\text{mg}\cdot\text{L}^{-1}$	$\text{K}^{+}$ $\text{mg}\cdot\text{L}^{-1}$	$\text{Ca}^{2+}$ $\text{mg}\cdot\text{L}^{-1}$	$\text{Mg}^{2+}$ $\text{mg}\cdot\text{L}^{-1}$	$\text{F}^{-}$ $\text{mg}\cdot\text{L}^{-1}$
S1	5.91	1714	1.4	7.0	1311.7	3	1.4	271.6	83	0.11
S2	5,87	1699	1.0	8.2	1230.7	2.9	1.5	266	80.5	0.08
S3	5.89	1614	2.8	10.3	1180.5	3.5	1.4	259.9	71.3	0.18
S4	5.95	1567	3.5	14.6	1150.3	5	1.8	253	68.9	0.10
S14	6,23	1740	6.4	9.0	1327	5.3	1.8	307	76.4	0.12
S20	6.19	1883	6.4	11.5	1342	5.9	3.40	306	76.9	0.14
S30	6.13	1679	3.65	15.8	1220	4.3	2.93	262	87.5	0.19
RSD* (%)			0.3062	0.3078		0.3280	0.3371	0.1650	0.2233	0.4698

\* It refers to the standard deviation of the chromatographic determinations for each anion and cation.

The concentration of ammonium ions was not analyzed in all 30 samples, for this reason the maximum, minimum and average values are presented only in Table 8.

**Table 8. The maximum, minimum and average values of the main physico-chemical parameters of natural mineral waters studied in a 30-month period**

Sample	The chemical parameter	Min	Max	Average
S1– S30	<i>pH</i>	5.87	6.23	6.05
	C.e. ( $\mu\text{S}\cdot\text{cm}^{-1}$ )	1567	1883	1743.6
	$\text{Cl}^{-}$ ( $\text{mg}\cdot\text{L}^{-1}$ )	1	7.4	4.98
	$\text{SO}_4^{2-}$ ( $\text{mg}\cdot\text{L}^{-1}$ )	7	24.3	12.37
	$\text{HCO}_3^{-}$ ( $\text{mg}\cdot\text{L}^{-1}$ )	1311.7	1355	1326.96
	$\text{Na}^{+}$ ( $\text{mg}\cdot\text{L}^{-1}$ )	2.9	6.4	4.72
	$\text{K}^{+}$ ( $\text{mg}\cdot\text{L}^{-1}$ )	1.4	3.4	2.30
	$\text{NH}_4^{+}$ ( $\text{mg}\cdot\text{L}^{-1}$ )	0.05	0.45	0.25
	$\text{Ca}^{2+}$ ( $\text{mg}\cdot\text{L}^{-1}$ )	253	311	287.82
	$\text{Mg}^{2+}$ ( $\text{mg}\cdot\text{L}^{-1}$ )	73	85	77.23
	$\text{CO}_2$ ( $\text{g}\cdot\text{L}^{-1}$ )	3.30	4.50	3.90
	$\text{NO}_3^{-}$ ( $\text{mg}\cdot\text{L}^{-1}$ )	0.1	3.95	2.71

Sample	The chemical parameter	Min	Max	Average
	Dry residue (mg·L <sup>-1</sup> )	158	191	173.33

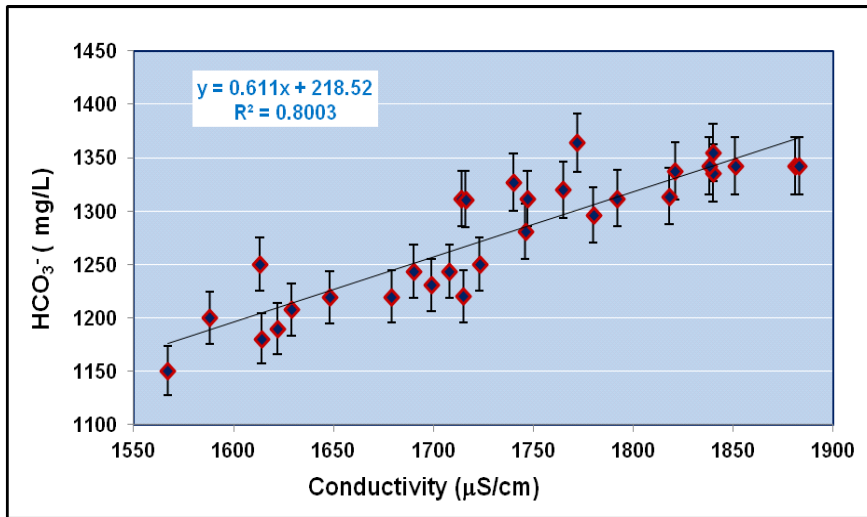


**Figure 10.** Dependence of HCO<sub>3</sub><sup>-</sup> (mg·L<sup>-1</sup>) concentration depending on the electrical conductivity (µS·cm<sup>-1</sup>) for the data set studied.

It can be seen from Figure 10 that the electrical conductivity values of the analyzed water samples are high, also indicating high ionic strength values due to hydrogeochemical dissolution in the presence of ions HCO<sub>3</sub><sup>-</sup>.

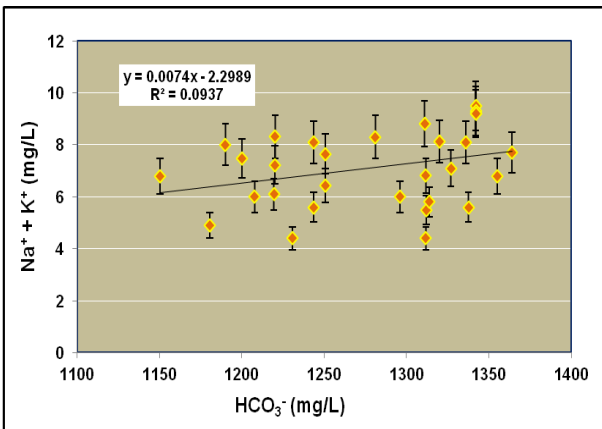


**Figure 13.** Dependence of

Na<sup>+</sup> și K<sup>+</sup> ion concentration (mg·L<sup>-1</sup>) depending on the concentration of the ion HCO<sub>3</sub><sup>-</sup> (mg·L<sup>-1</sup>).

The concentrations of alkali metals ions present in these systems are randomly correlated with the concentration of HCO<sub>3</sub><sup>-</sup> ions (Figure 13), the data obtained showing a large excess of HCO<sub>3</sub><sup>-</sup> ions compared to Na<sup>+</sup> și K<sup>+</sup> ions, which does not depend on the season.

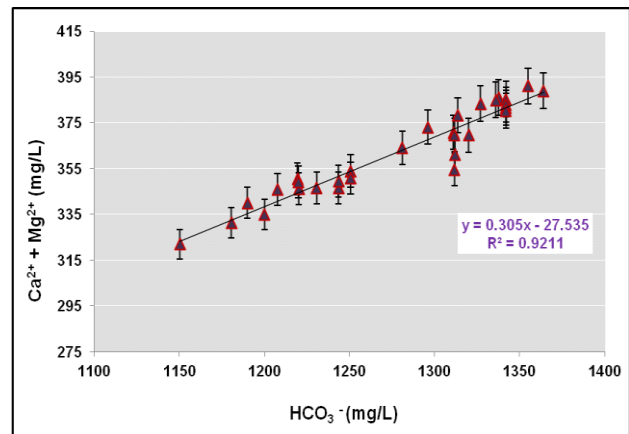


**Figure 14.** Dependence of

Ca<sup>2+</sup> și Mg<sup>2+</sup> ions concentration (mg·L<sup>-1</sup>) depending on the concentration of the ion HCO<sub>3</sub><sup>-</sup> (mg·L<sup>-1</sup>).

The correlation between the concentrations of alkaline earth metal ions and the concentration of HCO<sub>3</sub><sup>-</sup> ions shows a linear dependence (Figure 14), with a higher correlation coefficient, suggesting higher concentrations of these Ca<sup>2+</sup>, Mg<sup>2+</sup> and HCO<sub>3</sub><sup>-</sup> species in the source rocks and a more good correlation between their concentrations.

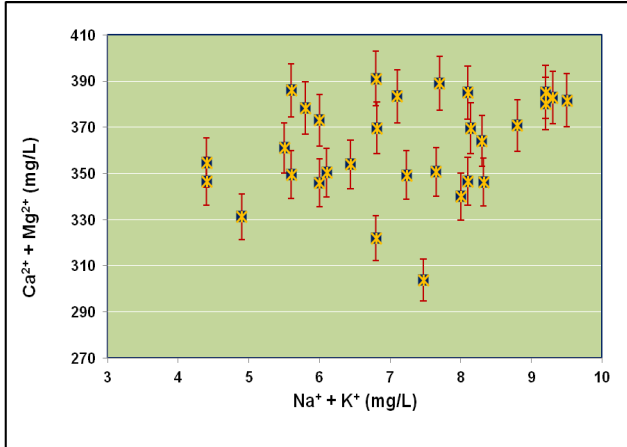


**Figure 15.** Dependence of  $\text{Ca}^{2+}$  și  $\text{Mg}^{2+}$  ions ( $\text{mg}\cdot\text{L}^{-1}$ ) vs.  $\text{Na}^+$  și  $\text{K}^+$  ( $\text{mg}\cdot\text{L}^{-1}$ ) in the studied systems.

The dependence of alkaline-earth metal ion concentrations on alkaline metal ion concentrations shows a dispersed distribution, specific to mineralized natural waters. The sum of the concentrations of  $\text{Na}^+$  and  $\text{K}^+$  ions is much lower than those of  $\text{Ca}^{2+}$  and  $\text{Mg}^{2+}$  ions, with  $\text{K}^+$  ions accounting for less than 2% in all samples, due to both rock erosion and the high  $\text{CO}_2$  content in the seepage water in the aquifer.<sup>7</sup>

As a result, nitrogen compounds such as ammonium, nitrate and nitrite ions show lower concentrations, indicating reduced pollution risks.<sup>8</sup>

The origin of ammonium ions in groundwater is based on complex, chemical and hydrogeochemical processes, influences of hydrogeological factors, partially taking into account potential sources of pollution.<sup>9</sup> In aqueous environments,  $\text{NH}_3$  is more toxic than  $\text{NH}_4^+$ , but in the range of  $\text{pH}$  values between 5.7 and 6.2 there is mainly the ionic form, respectively in the form of  $\text{NH}_4^+$  ions.<sup>10</sup> At a  $\text{pH}$  value of 9.3, ammonia is present in a percentage of 50% in aqueous solutions, and for  $\text{pH}$  values lower than 8.0, the percentage concentration of ammonia drops below 4.5%.<sup>11</sup>

The natural carbonated mineral waters studied do not present high concentrations of nitrogenous species, their low values being due to the depth of the aquifer, the impermeable rocks that make it up excluding the appearance of nitrogenous species from organic matter in surface and rainwater.

### 3.3.2. Results of radiometric analyses

Gross-alpha and gross-beta activity concentrations and effective annual doses for the 30 samples analyzed and presented in Table 7, the values for gross-alpha activity are in the range of  $1.03 - 5.50 \text{ mBq}\cdot\text{L}^{-1}$  and in range  $15.9 - 31.40 \text{ mBq}\cdot\text{L}^{-1}$  for gross-beta activity. Although the measurements were performed on samples collected over a longer period of time, the values of alpha and beta activity concentrations vary, showing differences of order of magnitude.

**Table 9.** Gross-alpha and gross-beta activity concentration values and of the effective annual doses of the analyzed natural mineral water samples

Sample	Residue average value	Gross- $\alpha$ average	Gross- $\beta$ average	Average annual effective dose DEFF
	$[\text{g}\cdot\text{L}^{-1}]$	$[\text{mBq}\cdot\text{L}^{-1}]$		$[\mu\text{Sv}\cdot\text{an}^{-1}]$
S1 ÷ S9	0.9167	$5.50 \pm 0.70$	$21.40 \pm 4.80$	33.95
S10 ÷ S17	1.5022	$2.40 \pm 1.30$	$15.90 \pm 5.40$	47.38
S18 ÷ S25	1.1229	$1.03 \pm 0.16$	$31.40 \pm 3.11$	15.45
S26 ÷ S30	1.1296	$4.56 \pm 1.30$	$28.34 \pm 7.70$	41.23

All values are lower than the reference concentration of the annual effective dose allowed by  $\mu\text{Sv}\cdot\text{an}^{-1}$ , but the concentration of radon present in the samples was not included.

**Table 10. The activity concentration values of  $^{40}\text{K}$ ,  $^{238}\text{U}$ ,  $^{232}\text{Th}$  and  $^{226}\text{Ra}$  in the residues of the analyzed water samples**

Sample/code	Average $^{40}\text{K}$	Average $^{238}\text{U}$	Average $^{232}\text{Th}$	Average $^{226}\text{Ra}$
	[Bq·L <sup>-1</sup> ]			
S1 ÷ S9	0.92 ± 0.11	0.055 ± 0.006	0.028 ± 0.003	0.28 ± 0.03
S10 ÷ S17	<0.53 (MDA)	0.084 ± 0.008	<0.012 (MDA)	0.45 ± 0.05
S18 ÷ S25	0.55 ± 0.06	0.12 ± 0.02	0.012 ± 0.002	0.11 ± 0.02
S26 ÷ S30	0.87 ± 0.08	0.21 ± 0.06	0.086 ± 0.010	0.280 ± 0.006
Medie ± 1σ	0.79 ± 0.08	0.12 ± 0.02	0.042 ± 0.005	0.28 ± 0.03
Range [Bq·L <sup>-1</sup> ]	MDA – 0.92 ± 0.11	0.055 ± 0.006 – 0.21 ± 0.06	MDA – 0.086 ± 0.010	0.11 ± 0.02 – 0.45 ± 0.05

MDA – Minimum Detectable Activity.

From the results presented in the literature, the activity concentration values of the analyzed radionuclides vary from the order of units in mBq·L<sup>-1</sup> to 1 Bq·L<sup>-1</sup> for  $^{40}\text{K}$ , while for  $^{238}\text{U}$  they vary from a few mBq·L<sup>-1</sup> (order of units) up to several hundreds of Bq·L<sup>-1</sup>.<sup>12</sup>

This study presents a new set of data on the radiochemical composition of mineral waters in Romania.

Variations in the concentrations of radionuclides  $^{40}\text{K}$ ,  $^{238}\text{U}$ ,  $^{232}\text{Th}$  and  $^{226}\text{Ra}$  indicate that, although the origins of these water samples are the same, they come from different depths and pass through different geological layers. The application of radiometric spectrometry methods to determine the activity of radionuclides provides valuable information regarding the transport of water between layers, surface or deep.

### Chapter 4. Chromatographic determination of nitrogen species from natural mineral waters by ion chromatography

Nitrogen is one of the elements that occur predominantly in nature and that form inorganic ionic species: nitrate, nitrite and ammonium. The maximum concentration of ammonium ions allowed in natural waters is  $0.5 \text{ mg}\cdot\text{L}^{-1}$ .<sup>11</sup>

If  $\text{NH}_4^+$  ions come into contact with oxygen, they transform into  $\text{NO}_2^-$  ions, which are then oxidized to  $\text{NO}_3^-$  ions. Drinking water is an important source of nitrate ions in the body, 10% of the daily dose of nitrates ingested, i.e. approximately 100 mg, comes from the water we drink.<sup>13</sup> The maximum nitrate concentration allowed in drinking water in most countries is  $50 \text{ mg}\cdot\text{L}^{-1}$ . Efficient separations can be achieved using eluents with appropriate compositions, flow rates related to the nature of the components to be separated, and stationary phases and detectors suitable for the type of separation (Table 13).

**Table 13. Examples of ion chromatography applications for the determination of ammonium ions**

Sample Matrix	Column	Eluent	Detector	Reference
Mineral water	IC-PAK CMD	$\text{HNO}_3 + \text{EDTA}$	Conductivity	<sup>14</sup>
Rain water	IC-PAK CM/D	$\text{HNO}_3 + \text{EDTA}$	Conductivity	<sup>15</sup>
Drinking water	Rapid cation	$\text{HCl} + 2,3\text{-diaminopropionic acid}$	Conductivity	<sup>16</sup>
Rain water	Dionex IonPac CS2	$\text{HCl}$	Conductivity	<sup>17</sup>
Drinking water	Dionex IonPac CS16	acid metansulfonic	Conductivity	<sup>18</sup>
Rain water	Dionex IonPac CS12A	$\text{H}_2\text{SO}_4$	Conductivity	<sup>19</sup>
Natural water	Dionex IonPac CG10 + CG10	$\text{HCl}$	Conductivity	<sup>20</sup>

A classic conductivity detector was used, both for cations and for anions, the mobile phase being a mixture of  $\text{Na}_2\text{CO}_3$  and  $\text{NaHCO}_3$  for anions and  $\text{HNO}_3$  and dipicolinic acid for cations, with a flow between  $0.7 \text{ mL}\cdot\text{min}^{-1}$  and  $0.9 \text{ mL}\cdot\text{min}^{-1}$ , to obtain optimal operating conditions.<sup>21</sup>

The purpose of the applied method was to analyze the  $\text{NO}_3^-$  and  $\text{NO}_2^-$  anions present at low concentrations in mineral waters, as well as to determine the concentration of  $\text{NH}_4^+$  ions, using the SR EN ISO 10304-1:2009 and SR EN ISO 14911:2003 standards. An anion suppression system was also used in order to optimize the analytical method in terms of accuracy, precision and total uncertainty.

The validated method was applied to a range of concentrations between 1 and  $100 \text{ }\mu\text{g}\cdot\text{L}^{-1}$  for fluoride, nitrite, bromide, nitrate and phosphate ions and between 100 and  $10,000 \text{ }\mu\text{g}\cdot\text{L}^{-1}$  for chloride and sulfate ions and for all cations, taking into account the matrices of the studied natural waters, being characterized three different concentration levels, to cover the minimum, average and maximum concentration values characteristic of natural mineral waters, and the determined parameters were: linearity range, determination of detection and detection limits quantification, precision, accuracy and uncertainty of the optimized method.

### 4.3. Results and discussion

The proposed method for the chromatographic determination of anions by ion chromatography with suppression shows better detection limits, compared to the standardized chromatographic method for the analysis of anions in natural waters.

A Metrosep A Supp 5-250/4.0 chromatographic column was used to improve the detection limit of the  $\text{NO}_3^-$  anion from  $0.1 \text{ mg}\cdot\text{L}^{-1}$  to  $0.01 \text{ mg}\cdot\text{L}^{-1}$  and the efficient separation of nitrite and nitrate anions. The elution process was isocratic, operating at a pressure of 7.95 MPa, the Metrosep column with a length of 250 mm instead of 150 mm, improving the separation.

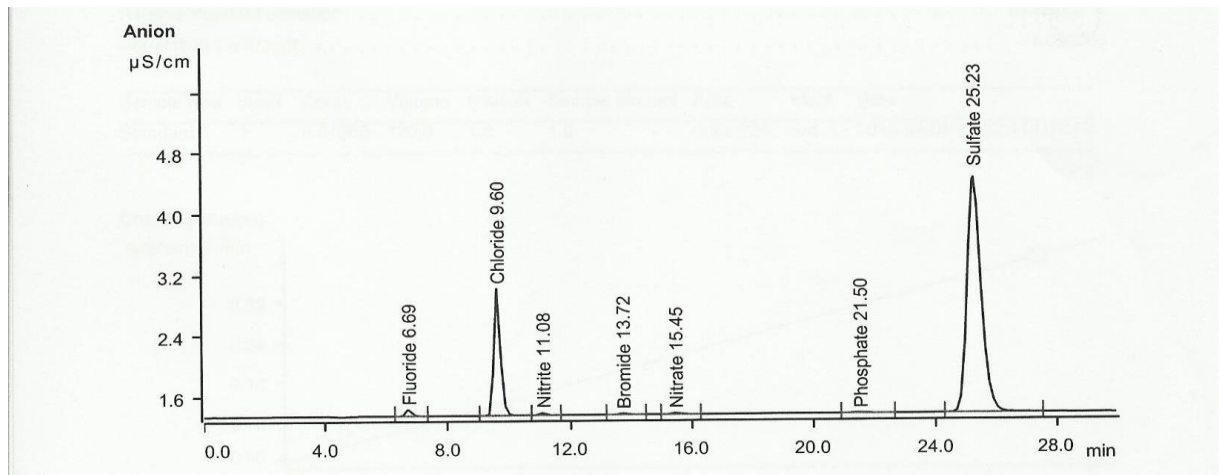


**Figure 17.** Chromatogram of a standard solution containing  $0.01 \text{ mg}\cdot\text{L}^{-1}$  of the anions: fluoride, chloride, nitrite, nitrate, phosphate and sulfate, using a Metrosep A Supp 5-250/4.0 column and an eluent with the composition:  $3.2 \text{ mM Na}_2\text{CO}_3$ ,  $1 \text{ mM NaHCO}_3$ , with a flow rate of  $0.7 \text{ mL}\cdot\text{min}^{-1}$ .

The total separation time was observed to be approximately 18 minutes using the Metrosep A Supp 5-150/4.0 column. For a column with a length of 250 mm, the total time required for the separation of anions is 26 minutes (Figure 17), but the detection limit of the method is better and the difference between the retention times of nitrogen ions and nitrogen ions allows the calculation of their concentrations without errors.

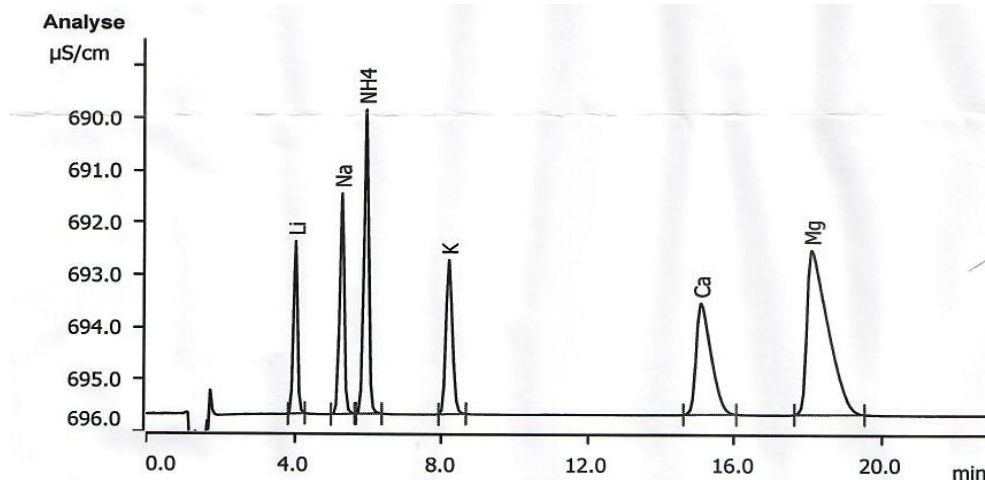


**Figure 18.** Chromatogram of a standard solution containing  $0.1 \text{ mg}\cdot\text{L}^{-1}$  each of the cations: lithium, sodium, ammonium, potassium, calcium and magnesium, using a Metrosep column C4- 150/4.0; eluent:  $1.7 \text{ mM}$  nitric acid and  $0.7 \text{ mM}$  dipicolinic acid, flow rate -  $0.9 \text{ mL}\cdot\text{min}^{-1}$ .

**Table 14. Calibration curve equations, relative standard deviations and correlation coefficients for: fluoride, chloride, nitrite, nitrate, phosphate and sulfate. Analytical conditions: column Metrosep A Supp 5-250/4.0, eluent: 3.2 mM Na<sub>2</sub>CO<sub>3</sub> and 1 mM NaHCO<sub>3</sub>, flow rate - 0.7 mL·min<sup>-1</sup>**

Anion	t <sub>R</sub> , min	The equation of the line	R <sup>2</sup>	RSD, %
F <sup>-</sup>	6.693	$y = -2.09371 \times 10^3 + 0.0164607x + 8.30169 \times 10^{-5}x^2$	0.999985	0.4698
Cl <sup>-</sup>	9.597	$y = -0.110065 + 0.0131663x + 4.39382x^2$	0.999998	0.3062
NO <sub>2</sub> <sup>-</sup>	11.082	$y = -7.05699 \times 10^{-5} + 6.22572 \times 10^{-3}x + 2.29263 \times 10^{-5}x^2$	0.999995	0.3371
Br <sup>-</sup>	13.722	$y = 1.48001 \times 10^{-4} + 4.04074 \times 10^{-3}x + 7.53939 \times 10^{-6}x^2$	0.999998	0.2333
NO <sub>3</sub> <sup>-</sup>	15.452	$y = 1.85857 \times 10^{-4} + 5.01555 \times 10^{-3}x + 1.15782 \times 10^{-6}x^2$	0.999999	0.1650
PO <sub>4</sub> <sup>3-</sup>	21.495	$y = -4.77868 \times 10^{-5} + 2.68596 \times 10^{-3}x + 4.73948 \times 10^{-6}x^2$	0.999997	0.3280
SO <sub>4</sub> <sup>2-</sup>	25.227	$y = -0.277475 + 9.93729 \times 10^{-3}x + 1.73806 \times 10^{-8}x^2$	0.999996	0.3078

From Table 14 it can be seen that the relative standard deviation values (RSD %) are greater than 0.3% for fluoride, chloride, nitrate, phosphate and sulfate ions and that the RSD% values are less than 0.3% for bromide and nitrite, the length of the chromatographic column used influencing the value of this parameter at higher concentrations of anions. In the analyzed samples, it is observed that the concentration values of NO<sub>3</sub><sup>-</sup> and NO<sub>2</sub><sup>-</sup> ions are lower than those of other anions present in the samples such as SO<sub>4</sub><sup>2-</sup> and Cl<sup>-</sup> anions.

**Table 15. Calibration curve equations, relative standard deviations and correlation coefficients for: lithium, sodium, ammonium, potassium, calcium and magnesium. Analytical conditions: Metrosep C4 column – 150/4.0, eluent: nitric acid 1.7 mM and dipicolinic acid 0.7 mM, flow rate - 0.9 mL·min<sup>-1</sup>**

Cation	t <sub>R</sub> , min	Ecuatia dreptei (x10 <sup>-5</sup> x)	R <sup>2</sup>	RSD, %
Li <sup>+</sup>	5.354	$y = 0.108830 + 5.2387x$	0.99998	0.668
Na <sup>+</sup>	6.358	$y = 0.028311 + 1.4612x$	0.99998	0.695
NH <sub>4</sub> <sup>+</sup>	7.092	$y = 0.028825 + 1.6589x$	0.99998	0.673
K <sup>+</sup>	8.445	$y = 0.1119557 + 7.7811x$	0.99987	0.673
Ca <sup>2+</sup>	16.472	$y = 0.044311 + 1.34479x$	0.99987	0.862
Mg <sup>2+</sup>	20.011	$y = 0.0448898 + 2.6830x$	0.99985	1.130

From Table 15 it can be seen that the relative standard deviation values (RSD %) are greater than 0.7% for Ca<sup>2+</sup> and Mg<sup>2+</sup> ions. It is also observed that the RSD% values for Li<sup>+</sup>, Na<sup>+</sup>, NH<sub>4</sub><sup>+</sup>, K<sup>+</sup> ions are very close.

In the method proposed in the paper, the Metrohm CO<sub>2</sub> suppressor (MCS) removes CO<sub>2</sub> from the eluent flow, thus reducing the conductivity of the background signal, thus being able to reduce the injected sample volume and the sensitivity of the detected signal.

The limit of detection together with the limit of quantification of the method were determined for each ion based on the standard deviations of repeated measurements. It was observed that by increasing the length of the column from 150 mm to 250 mm, the sensitivity of the method does not decrease, and the separation of the peaks improves. After chemical suppression, a certain amount of dissolved CO<sub>2</sub> remains in the eluent, and its dissociation equilibrium changes very little during the separation, producing the baseline variation. That is why in ion chromatography with suppression the calibration curves are not linear, the quadratic regression improving the quality of the results.

**Table 16. The values of parameters for validation of the chromatographic method analysis of nitrate and nitrite ions**

Ion	Parameter	Low conc. 1 $\mu\text{g L}^{-1}$	Midle conc. 10 $\mu\text{g L}^{-1}$	High conc., 100 $\mu\text{g L}^{-1}$
$\text{NO}_2^-$	Repeatability,	2.00	1.92	2.44
	Recovery rate, %	109.8	95.60	91.40
	Limit of detection, $\mu\text{g}\cdot\text{L}^{-1}$		1.06	
	Limit of quantification, $\mu\text{g}\cdot\text{L}^{-1}$		3.24	
	RSD %		0.65	
	Total uncertainty %		15.00	
$\text{NO}_3^-$	Repeatability,	2.67	3.89	0.89
	Recovery rate, %	115.9	99.84	84.13
	Limit of detection, $\mu\text{g}\cdot\text{L}^{-1}$		1.09	
	Limit of quantification, $\mu\text{g}\cdot\text{L}^{-1}$		3.27	
	RSD %		0.80	
	Total uncertainty %		10.00	

The accuracy and precision of the method on the three concentration ranges are presented in Table 16, the precision being determined based on the resumption of the procedures, calculated from the repeated analyzes. The total uncertainty combines the concentration uncertainty of the standard solutions, the uncertainty of the calibration curve and the uncertainty of the conductivity measurements in accordance with detector specifications, a total uncertainty value of 15% being accepted for low concentration levels.

**Table 17. Results for LoD and LoQ of the chromatographic method for nitrogen analysis from drinking water – 10 samples enriched with 40 mL  $\text{NH}_4^+$  standard (0,005  $\text{mg}\cdot\text{L}^{-1}$ )**

Sample	$\mu\text{g}$ of nitrogen in a 50 mL volumetric flask		
Sample 1	0.1679		
Sample 2	0.1236		
....	...		
Sample 9	0.1915		
Sample 10	0.1387		
Average value (X)	0.1533		
Standard deviation (s)	0.025		
3s	0.075		
10s	0.25		
		$\mu\text{g N}$	$\mu\text{g N/mL}$
LoD	X+3s	0.2283	0.0046
LoQ	X+10s	0.4033	0.008

Values considered:

- LoD = 0.2283  $\mu\text{g N}$  in the solution in the flask by 50 mL or solution of 0.0046  $\mu\text{g N/mL}$ ;
- LoQ = 0.4033  $\mu\text{g N}$  in the solution in the flask by 50 mL or solution of 0.008  $\mu\text{g N/mL}$ .

Detection limit and quantification limit in  $\text{mg NH}_4^+/\text{L}$ , so LoD and LoQ is:

- LoD = 0.0046 x 1.288 = 0.0059  $\text{mg NH}_4^+/\text{L}$  water;
- LoQ = 0.008 x 1.288 = 0.0103  $\text{mg NH}_4^+/\text{L}$  water.

All analyzed samples showed low or medium values of mineralization, reflecting the composition of the rocks from which the natural waters provided.

**Table 18. Chemical composition of the analyzed natural waters**

Sample	HCO <sub>3</sub> <sup>-</sup> mg·L <sup>-1</sup>	Mineralization mg·L <sup>-1</sup>	NO <sub>3</sub> <sup>-</sup> mg·L <sup>-1</sup>	NO <sub>2</sub> <sup>-</sup> mg·L <sup>-1</sup>	Cl <sup>-</sup> mg·L <sup>-1</sup>	SO <sub>4</sub> <sup>2-</sup> mg·L <sup>-1</sup>	Na <sup>+</sup> mg·L <sup>-1</sup>	Ca <sup>2+</sup> mg·L <sup>-1</sup>	Mg <sup>2+</sup> mg·L <sup>-1</sup>	NH <sub>4</sub> <sup>+</sup> mg·L <sup>-1</sup>
1	219.6	278.8	0.80	< 0.01	0.45	6.76	0.75	48.33	15.20	0.22
2	1281.2	1684	0.034	<0.01	4.9	19.45	4.33	290	82.5	0.40
3	-	-	2.3	< 0.01	0.15	7.66	0.98	66.86	2.88	-
4	333.4	462.7	4.11	-	1.08	10.38	2.85	56.73	32.5	0.24
8	312	485	2.07	< 0.01	0.80	13.39	1.7	94.5	7.8	0.25

The method validated in this paper was applied to several categories of natural mineral waters, using standard multianion and multication solutions.

The method for anions can be applied for the concentration ranges:

- 100-10000 µg·L<sup>-1</sup> for anions Cl<sup>-</sup> și SO<sub>4</sub><sup>2-</sup>
- 1-100 µg·L<sup>-1</sup> for anions F<sup>-</sup>, Br<sup>-</sup>, NO<sub>2</sub><sup>-</sup>, NO<sub>3</sub><sup>-</sup> și PO<sub>4</sub><sup>3-</sup>.

The method for cations can be applied for the concentration range 100-10000 µg·L<sup>-1</sup>.

The methods present the possibility of analyzing some ionic species at very low concentrations, in matrices with compositions with large differences in the values of the concentrations of the ionic species present, depending on the nature of the rock deposits from which they come and sometimes also on the extremely low pollution.

Following the improvement of the experimental conditions in the method for determining nitrogen species in samples, the quantification limits for NO<sub>3</sub><sup>-</sup> and NO<sub>2</sub><sup>-</sup> anions were reduced 10 times using:

- suppression chromatographic method,
- a chromatographic column of 250 mm, longer Metrosep,
- a degassing treatment before starting the actual analysis.

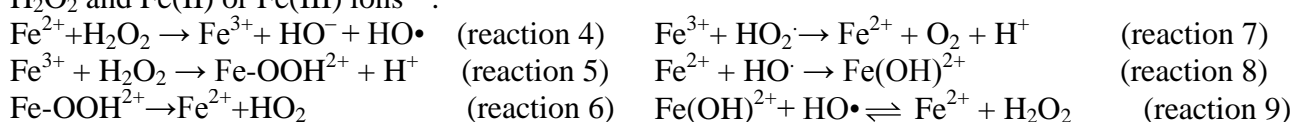
Limits of quantification of some ions can be reduced by reducing injection volumes and by reducing contamination. However, further processing steps are needed to develop an improved analytical method validated for traces of NO<sub>3</sub><sup>-</sup> and NO<sub>2</sub><sup>-</sup> in the presence of higher concentrations of Cl<sup>-</sup>, SO<sub>4</sub><sup>2-</sup> and CO<sub>3</sub><sup>2-</sup> ions in the samples.

The method of analysis of ammonium ions was separation chromatography of cationic species, obtaining its improvements due to the prior degassing of the samples subjected to analysis and the use of small injection volumes of 2 µL. These were reflected in the symmetrical appearance of the chromatographic peaks and the reduced background noise.

## Chapter 5. The distribution of some nitrogen species during the processes washing of natural mineral water bottling installations

Among the natural water treatment methods is the Fenton method, which represents an effective alternative to the conventional biological decontamination treatments of natural waters<sup>22</sup>, optimized over the years.<sup>23</sup> In the presence of traces of H<sub>2</sub>O<sub>2</sub>, used especially as a disinfectant, the Fenton-type reaction leads during microbial degradation to the oxidation of ammonium ions, with the formation of NO<sub>3</sub><sup>-</sup> and NO<sub>2</sub><sup>-</sup> ions, which influences the variations in their concentrations in natural mineral waters<sup>24</sup>, in which the Fenton-type reaction can occur in the presence of Fe<sup>2+</sup> in combination with H<sub>2</sub>O<sub>2</sub> from various sources.<sup>25</sup>

The generation of HO• radicals in the Fenton-type reaction is due to the interaction between H<sub>2</sub>O<sub>2</sub> and Fe(II) or Fe(III) ions<sup>26</sup>:



The transformation of nitrogen compounds from natural mineral waters consists in the oxidation process of ammonium ions, resulting NO<sub>3</sub><sup>-</sup> ions that are formed in the presence of H<sub>2</sub>O<sub>2</sub> used in oxidative treatment methods. The presence of Fe<sup>2+</sup> ions, naturally in the matrices of natural mineral waters, increases the oxidation yield of ammonium, which is mainly transformed into nitrate ions. For pH values between 5.5 and 6.0, NH<sub>4</sub><sup>+</sup> ions are mainly found in carbonated natural mineral waters, at normal temperatures. Under aerobic conditions, NH<sub>4</sub><sup>+</sup> ions are transformed into NO<sub>3</sub><sup>-</sup> ions in two stages:



Since natural carbonated mineral waters naturally contain Fe<sup>2+</sup> ions that are partially removed by deferrization and demanganization processes, these in contact with H<sub>2</sub>O<sub>2</sub>, used in the oxidative treatment methods of natural waters will naturally generate an in-situ Fenton type system, which leads to the modification of the concentration distribution of nitrogen species in the matrices during the water treatment processes.

Considering the impact of pH on the possible transformations of nitrogen species in the presence of Fe<sup>2+</sup> ions and H<sub>2</sub>O<sub>2</sub>, the variations in the concentrations of NH<sub>4</sub><sup>+</sup>, NO<sub>3</sub><sup>-</sup> and NO<sub>2</sub><sup>-</sup> ions were monitored, also taking into account the presence of Cl<sup>-</sup> and SO<sub>4</sub><sup>2-</sup> ions in important concentrations in these matrices. In the experiments carried out, the concentrations of the main inorganic cations and anions were analyzed monthly, during four seasons, the values used in the calculations representing the average of the values obtained as a result of the monitoring.

The initial values of pH, electrical conductivity and concentrations of NH<sub>4</sub><sup>+</sup>, Fe<sup>2+</sup>, Cl<sup>-</sup> and SO<sub>4</sub><sup>2-</sup> ions were determined from samples with volumes of 20 mL, before the addition of volumes of H<sub>2</sub>O<sub>2</sub>, in the oxidative treatment processes. Correlated with the initial composition of natural mineral waters, the concentrations of ionic species with nitrogen were determined after predetermined contact times: NH<sub>4</sub><sup>+</sup>, NO<sub>3</sub><sup>-</sup> and NO<sub>2</sub><sup>-</sup>, for five hours, using chromatographic methods for the analysis of anions and cations for ions NH<sub>4</sub><sup>+</sup>, Fe<sup>2+</sup>, NO<sub>2</sub><sup>-</sup> și NO<sub>3</sub><sup>-</sup>.<sup>27</sup> The water samples have compositions similar to those analyzed previously.

### 5.3. Results and discussion

The methods of treating natural mineral waters through oxidative processes can generate Fenton systems in the presence of Fe<sup>2+</sup> ions, naturally present in these waters. The purpose of the

oxidative treatment methods is to remove possible microbiological contamination of the transport pipes of the water sources, as well as of their collection installations, in accordance with national and European regulations.<sup>28</sup>

The chosen method allows the systematic study of the variables that can contribute significantly during the applied oxidative processes. In the experimental conditions chosen, the effect of the concentration of  $\text{H}_2\text{O}_2$ , used as an oxidizing agent, was studied, the evolution of the concentration being analyzed at intervals of 10 minutes, for one hour, the duration of time allowed in the oxidative treatment processes. In the analyzed samples, the initial concentrations of  $\text{NO}_3^-$  and  $\text{NO}_2^-$  ions can be determined by the chromatographic method used.

The initial composition of the analyzed samples is taken into account, monitoring at regular intervals the concentrations of  $\text{Fe}^{2+}$  and  $\text{NH}_4^+$  ions, as well as the concentration of  $\text{H}_2\text{O}_2$  in the studied samples and determining the range of values in which they can vary.

In Table 21, the control experiments performed show that the  $\text{H}_2\text{O}_2$  concentration values in the samples are sufficient to generate Fenton-type systems in the absence of other reagents. Under these conditions, the evolution of  $\text{Fe}^{2+}$ ,  $\text{NO}_2^-$ ,  $\text{NO}_3^-$ ,  $\text{NH}_4^+$  ions,  $\text{pH}$  and electrical conductivity is analyzed for 300 minutes, and the samples were analyzed chromatographically.

**Table 21. Variation of concentration of  $\text{H}_2\text{O}_2$  ( $C_i = 4 \text{ mg}\cdot\text{L}^{-1}$ ) during the water treatment process**

Time (minute)	Concentration $\text{H}_2\text{O}_2$ ( $\text{mg}\cdot\text{L}^{-1}$ )
0	4
10	3.5
20	3.1
30	2.5
40	2
50	1.8
60	1.8

The monitoring of nitrogen species concentrations was continued for five hours after the oxidative treatment of the waters, because it was found from previous studies that after this interval the entire amount of added oxygenated water was consumed.

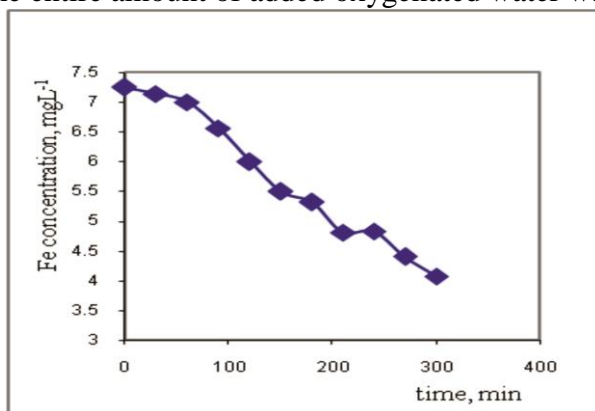


**Figure 20.** Variation of the concentration of  $\text{Fe}^{2+}$  ions in natural carbonated mineral waters, the concentration of divalent iron ( $7.25 \text{ mg}\cdot\text{L}^{-1}$ ) oxidatively treated with a  $\text{H}_2\text{O}_2$  solution of concentration  $2.0 \text{ mg}\cdot\text{L}^{-1}$ , at a contact time of 6 hours.

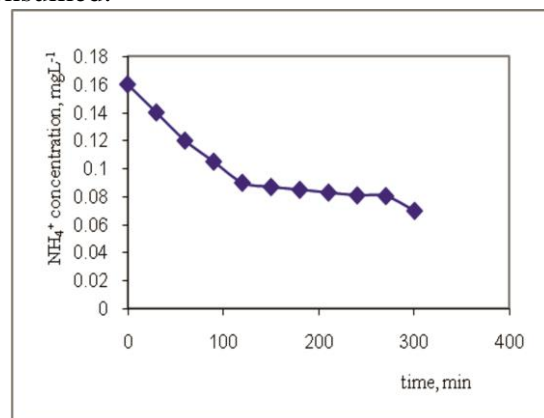


**Figure 21.** Variation of ammonium ion concentration in natural carbonated mineral waters, initial concentration of  $\text{NH}_4^+$  ( $0.16 \text{ mg}\cdot\text{L}^{-1}$ ), initial concentration of  $\text{H}_2\text{O}_2$  ( $2.0 \text{ mg}\cdot\text{L}^{-1}$ ), at a contact time of 6 hours.

It can be seen from Figure 20 the decrease in the concentration of  $\text{Fe}^{2+}$ , in the Fenton-type system generated in the matrix of natural mineral waters, in the presence of  $\text{H}_2\text{O}_2$ . The  $\text{Fe}^{2+}$  ions initially present in the aqueous matrix are oxidized to  $\text{Fe}^{3+}$ , in the presence of oxygenated water, accumulating in the system<sup>29</sup> and being subsequently removed through the deferrization/demanganese process. Under these conditions, the Fenton reaction shows higher yields in the presence of  $\text{Fe}^{2+}$  ions, compared to the slower oxidation process and lower yields in the presence of  $\text{Fe}^{3+}$  ions.

The influence of  $\text{H}_2\text{O}_2$  concentration on the concentration distribution of nitrogen species was studied, the variation of its concentration being the critical variable of the process.<sup>30</sup>

Figure 21 shows the variation in the concentration of  $\text{NH}_4^+$  ions in carbonated natural mineral waters.

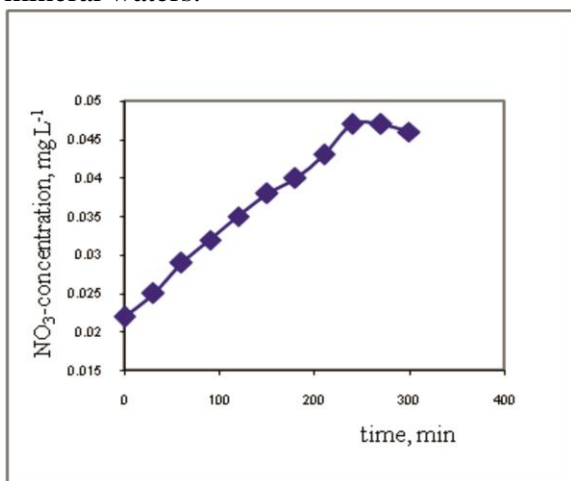


**Figure 22.** The variation of the nitrogen ion concentration in natural carbonated mineral waters, which contain an initial concentration of  $\text{NH}_4^+$  ions of  $0.16 \text{ mg}\cdot\text{L}^{-1}$  treated with a  $\text{H}_2\text{O}_2$  solution of concentration  $2.0 \text{ mg}\cdot\text{L}^{-1}$ , at a treatment time of one hour and monitoring time 6 hours.

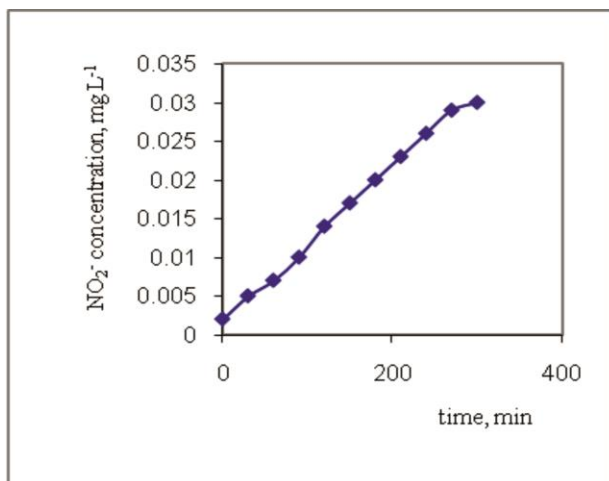


**Figure 23.** The variation of the anion concentration nitrite in natural carbonated mineral waters, with an initial concentration of  $\text{NH}_4^+$  ions of  $0.16 \text{ mg}\cdot\text{L}^{-1}$ , treated oxidatively by the Fenton reaction with a solution of concentration  $2.0 \text{ mg}\cdot\text{L}^{-1}$   $\text{H}_2\text{O}_2$ , at a treatment time of one hour and a monitoring time of 6 hours.

In all experiments, the chosen concentration values were  $2.7 \text{ mg}\cdot\text{L}^{-1}$  for  $\text{Cl}^-$  and  $20.7 \text{ mg}\cdot\text{L}^{-1}$  for  $\text{SO}_4^{2-}$ , based on the concentration values of these ions following the annual monitoring. Figure 22 shows the variation of the  $\text{NO}_3^-$  concentration in the studied solutions that increased following the oxidative treatment based on the Fenton-type reaction. Taking into account the reactions in which  $\text{NH}_4^+$  ions are involved during the oxidative treatment, the concentrations of  $\text{NO}_3^-$  can increase up to the level of the initial concentration of  $\text{NH}_4^+$  in the samples of natural carbonated mineral waters.

In all experiments, the concentrations of  $\text{NO}_2^-$  ions could also be determined, their values not being below the detection limit of the chromatographic instrument. (Figure 23).

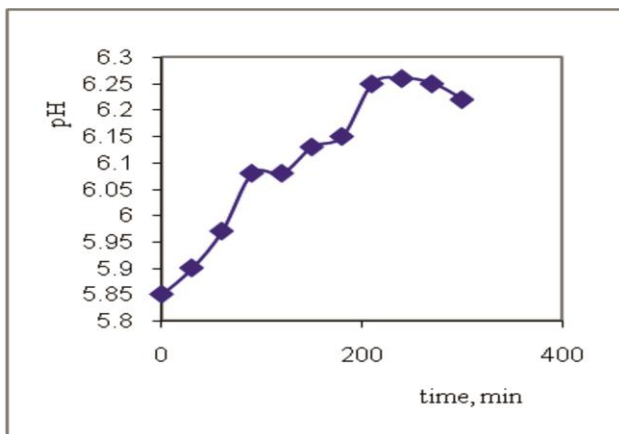


**Figure 24.** Variation of the  $pH$  of natural carbonated mineral waters, treated with a  $H_2O_2$  solution of concentration  $2.0 \text{ mg}\cdot\text{L}^{-1}$ , at a treatment time one hour and monitoring time 6 hours.

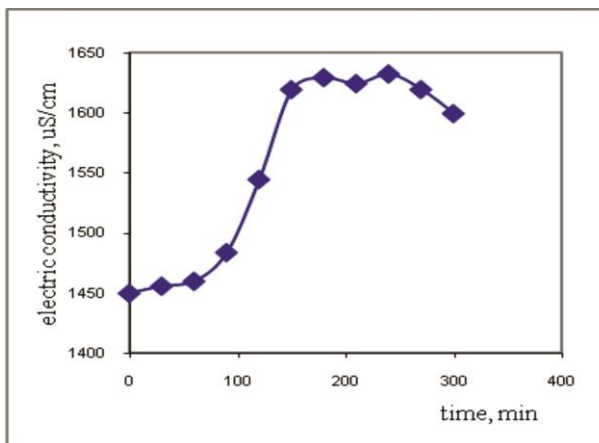


**Figure 25.** Variation of electrical conductivity of treated natural mineral carbonated waters with a  $H_2O_2$  solution of concentration  $2.0 \text{ mg}\cdot\text{L}^{-1}$ .

Figure 24 shows the variation of the  $pH$  values of the carbonated natural mineral water solution, for six hours, from an initial value of 5.85, following treatment with a  $H_2O_2$  solution of concentration  $2.0 \text{ mg}\cdot\text{L}^{-1}$ .

The  $pH$  evolution during the oxidative treatment initially shows a slight increase which could be due to the displacement of the carbonate ion balance, due to degassing by removing  $CO_2$  from the solution.<sup>31</sup> Another cause could be due to the consumption of  $H^+$  ions during the Fenton reaction, probably significantly influencing the  $pH$  variation of the analyzed samples.<sup>32</sup>

Following oxidative treatment processes with  $H_2O_2$  solutions of different concentrations, following which Fenton-type reactions take place, the  $pH$  values of the solutions may increase for the following reasons:

- bacterial degradation of nitrogen compounds, which can lead to the formation of alkaline secondary products;
- displacement of the equilibrium reaction of  $CO_2$  – carbonate by heating the aqueous solution and degassing  $CO_2$ ;
- oxidation of ammonium ions, initially present in natural mineral water matrices, to nitrate and nitrite.

The  $pH$  values become more alkaline during the Fenton-type process of oxidative treatment, an increase of 0.5 to one unit. This slight increase of  $pH$  values could be beneficial for naturally carbonated mineral waters, usually more acidic. The efficiency of the nitrite oxidation process with dissolved oxygen increases as the  $pH$  decreases ( $pH = 3.0 - 6.0$ ). This is due to the increase in the concentration of  $HNO_2$ , one of the compounds that appears at lower  $pH$  values. For  $pH$  values around 3.5, about 80% of the nitrite ions are oxidized to nitrate. For  $pH$  values  $> 6$ , the formation of the nitrogen anion is not observed.<sup>33</sup>

Figure 25 shows the variation of electrical conductivity of carbonated natural mineral waters. The higher values of electrical conductivity can be explained by the higher mobilities of oxidized nitrogen species, nitrate and nitrite compared to ammonium, nitrate and nitrite ions resulting from ammonium oxidation processes, compared to the initial concentration of ammonium ions in the samples.

This study revealed the existence of several types of nitrogen compounds following the Fenton type disinfection treatment in the collection tanks of carbonated natural mineral waters.

Several factors have been studied that influence the formation of nitrogen compounds that appear and the variation of their concentration distribution, among which:

The oxidation of  $\text{NH}_4^+$  ions ultimately leads to a decrease in their initial concentration, the concentration of nitrates increasing due to the oxidation of ammonium ions or the nitrification reactions of several microorganisms such as: nitrobacter and nitrosomonas bacteria. However, this increase remains very low, in direct correlation with both the initial ammonium concentration and the initial concentration of nitrogen species in the matrix.

The *pH* values increase after using  $\text{H}_2\text{O}_2$  as a sanitizing agent, but considering the slightly acidic initial *pH* value in carbonated mineral waters, this increase does not affect either the taste or the chemical composition of most compounds.

## **Chapter 6. Ammonium ion adsorption on nanoplatelets unmodified (pristine) and oxidized exfoliated graphite**

The applications of nanostructured carbon-based nanomaterials start from their properties:

- large specific surface area;
- possibilities of rapid dispersion and in controlled environments;
- high reactivity;
- great capacity to remove pollutants.<sup>34</sup>

Carbon-based nanomaterials are beginning to be used, especially in the last ten years<sup>35</sup>, as effective sorbents for the removal of contaminants from aqueous matrices, unmodified or modified graphene and carbon nanotubes have already been presented in the literature as having important sorption capacities for certain types of contaminants in natural waters, and the legislative limitations imposed on treatment technologies and associated infrastructures integrating them into installations and devices in drinking water supply systems.

Nanomaterials are applied in drinking water treatment in:

- adsorption-desorption processes,
- membrane, photocatalytic processes,
- disinfection treatments and microbial control detection processes,
- evaluation and monitoring of water sources before and after treatment.<sup>36</sup>

The role of surface chemistry was confirmed by previous studies on ammonium ion sorption using carbon-based nanomaterials<sup>37</sup>, but very few articles report data on ammonium adsorption on modified carbon-based nanomaterials, especially through oxidation, the applications of these advanced materials being still in the laboratory or pilot research stage, especially in terms of environmental applications.

There are several treatment methods that can be used (membrane purification, photocatalysis, ion exchange or combined methods), but adsorption processes have advantageous characteristics such as high contaminant removal efficiency, simple technological facilities and low energy consumption. In addition, treatments based on adsorption procedures are among the only treatments allowed for natural mineral waters, based on European legislation.

Simple and functionalized graphene, as well as simple and functionalized graphite nanoplatelets are used in these processes for the removal of organic and inorganic contaminants<sup>38</sup>, being mentioned in the literature processes of ammonium ion adsorption from natural waters based on acid-base interactions with the functional groups containing oxygen, located at the edges of the graphene layers.<sup>39</sup>

In this study were investigated:

- the characteristics of the ammonium adsorption process on pristine and oxidized exfoliated graphite nanoplatelets (xGnP), analyzing both the kinetics of the process and the adsorption isotherms, the experimental data being then modeled with different types of Langmuir, Freundlich, Temkin sorption models, Harkin-Jura and Halsey, based on the correlations between the equations of these models and the experimental data, establishing the correlation coefficients corresponding to each applied model.
- the thermodynamic and kinetic parameters were calculated to determine the adsorption mechanisms, studying the influences of several factors specific to natural aqueous samples (the influence of pH, the influence of temperature and the influence of the initial concentration of  $\text{NH}_4^+$ ).
- the characteristics of the adsorption process of ammonium ions on exfoliated (xGnP) and oxidized (ox-xGnP) graphite nanoplatelets were studied, the equilibrium data being modeled using

the Langmuir 2, Freundlich, Temkin and Harkins-Jura sorption isotherm equations in order to determine the correlation between experimental and calculated data.

The obtained results were compared with those in the literature, already reported in other studies of sorption of ammonium ions on activated carbon<sup>40,41</sup>, porous zeolites<sup>42</sup>, graphene and functionalized graphene<sup>43,44</sup>, more intense sorption processes being observed on oxidized graphene.<sup>45</sup> It was also observed that a higher porosity of the surfaces does not lead to superior adsorption of ammonium on the nanostructured surfaces.<sup>46</sup>

Graphene materials<sup>47,48,49</sup> and carbon nanotubes<sup>50</sup> show good adsorption capacities of some pollutants from aqueous environments, and by modifying them with different substituents they can acquire selectivities only towards certain species present in aqueous environments, for example the natural radionuclides present in these matrices.<sup>51</sup>

### 6.2.3. Methods of work

– The chromatographic method used was SR EN ISO 14911:2003 for the determination of cations in water;

– The specific surface of the sorbent was determined by measuring nitrogen adsorption-desorption isotherms, using the BET method at relative pressures ( $P/P_0$ ) in the range 0.0001-0.9900.

– The number and type of functional groups on the oxidized surfaces of xGnP were quantitatively estimated using the Boehm titration method, described in<sup>52</sup>, as well as the pH of the point of zero charge ( $pH_{PZC}$ ).

### 6.5. Exfoliated carbon nanoplatelets additionally oxidized as sorbents for ammonium ions

To quantify the concentration of acidic reaction centers, by Boehm titration<sup>53</sup>, different basic solutions with suitable  $pK_b$  values are used, which selectively react at the level of acidic centers with different dissociation constants,  $pK_a$ . Thus, NaOH solution is used as a titration reagent for phenolic carboxyl, carbonyl, and hydroxyl groups, and  $NaHCO_3$  is used as a titration reagent for carboxyl groups only.

The objective of this research was to study the adsorption process of ammonium ions using as sorbents - nanomaterials based on carbon, such as exfoliated graphite nanoplatelets (xGnP), oxidized with  $HNO_3$  with a reflux time of three hours.

#### 6.5.2.3. Adsorption experiments for samples

Analysis methods:

– for the determination of ammonium ions in all aqueous solutions, the chromatographic method

– the BET surface of xGnP and ox-xGnP was analyzed by nitrogen adsorption at the working temperature of 77 K, at which the adsorption-desorption isotherms were recorded, the samples being degassed in vacuum at 60 °C for 4 hours.

– the characterization of carbon-based nanomaterials was performed using Fourier transform infrared spectroscopy (FTIR) and scanning electron microscopy (SEM).

– the type and concentration of acidic functional groups on the surface obtained by oxidation were determined using the Boehm method.

– The zero charge point pH ( $pH_{PZC}$ ) was determined based on the pH variation method.<sup>54</sup>

### 6.5.3. Results and discussion

#### 6.5.3.1. Characterization of oxidized xGnP

##### 6.5.3.1.1. Fourier-transformed infrared spectra (FTIR)

To investigate the structure of ox-xGnP, Fourier transformed infrared (FTIR) spectrometry was used as the analysis method of xGnP and ox-xGnP doped with KBr, and the spectra are shown in Figure 44.

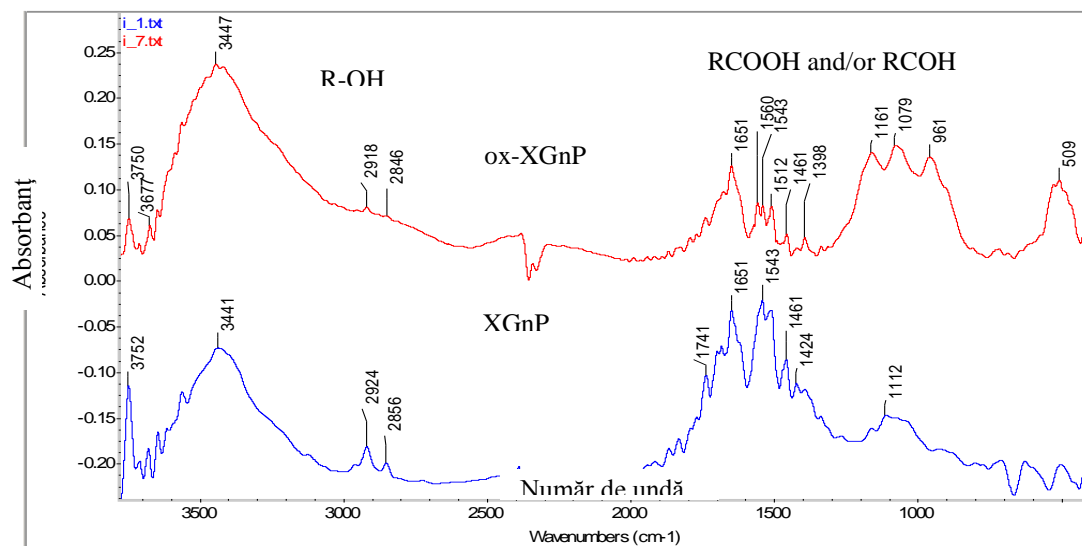


**Figure 44.** Fourier transformed infrared (FTIR) spectra of unoxidized xGnP (blue line) and oxidized xGnP (red line).

##### 6.5.3.1.2. Scanning Electron Microscopy (SEM)

In the investigations of xGnP microstructures and for their visualization, scanning electron microscopy (SEM) was used.

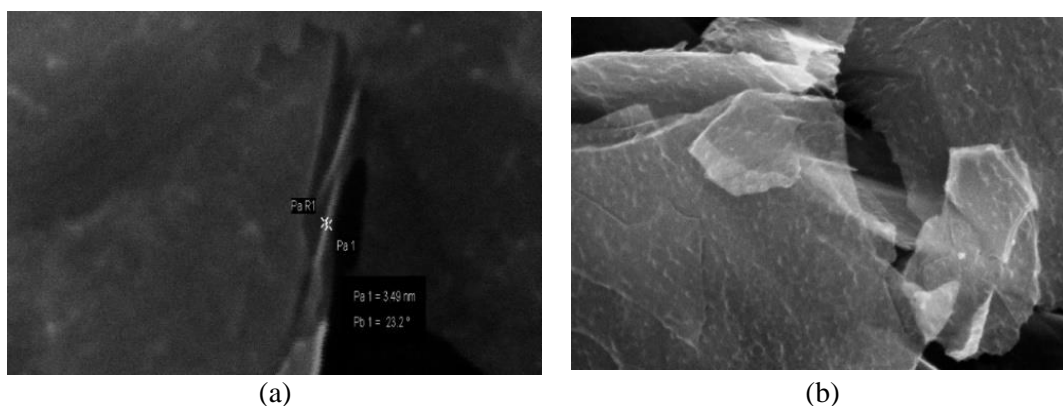


**Figure 45.** SEM images of xGnP (a) and ox-xGnP (b).

After oxidation of xGnP, oxygen-containing functional groups appeared at the edges of the surfaces (white spots). Also, the fragmentation of the sheets indicated that the oxidation process had taken place. The different acidic functional groups on the xGnP surface, such as phenolic carboxyl,

carbonyl and hydroxyl groups, resulting from oxidation conferred improved hydrophilic properties, increasing the degree of dispersion of ox-xGnP in aqueous media, compared to that of xGnP. If the pH of the working solution is higher than the zero charge pH, the total negative charge of the surface provides electrostatic interactions, favorable for the adsorption of positively charged species.

#### 6.5.3.1.4. Boehm titration

Acidic and basic functional groups were determined based on the Boehm titration method. The different acidic functional groups can be identified and quantified using sodium bicarbonate solutions to neutralize only the carboxyl groups and sodium carbonate solutions to neutralize the carboxyl and lactone groups. Based on this chemical behavior,  $\text{NaHCO}_3$  ( $pK_a = 10.25$ ) reacted with carboxyl groups ( $pK_a < 5$ ), but not with hydroxyl groups from phenols or alcohols ( $pH > 9$ ). Sodium hydroxide neutralizes the acid groups on the surface, the carboxyl, lactonic and phenolic groups. Different types of acidic functional groups were quantified using acid titration volume to determine  $\text{mmol H}_3\text{O}^+$  equivalent/g ox-xGnP.

For the determination of total acidic functional groups, the steps are shown in Figure 48.

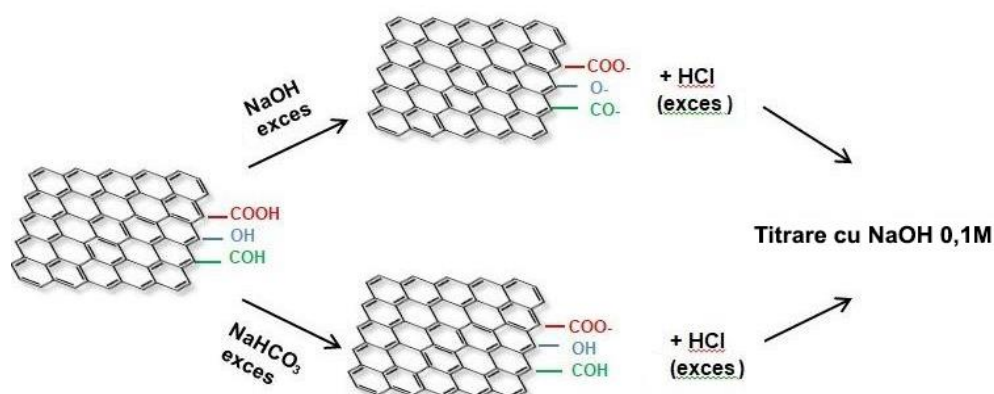


**Figure 48.** Scheme of the analytical method developed for the selective titration of total acidic functional groups and carboxyl groups created on the ox-xGnP surface.

It can be seen from Table 31 that the values of the concentrations of acid groups obtained by different oxidation methods differed depending on the reaction conditions, therefore it was necessary to determine each of them by several methods, the Boehm titration being one such method .

**Table 31.** Specific surface area, zero charge point pH, and number of oxidized functional groups on xGnP surface (ox-xGnP) determined by Boehm titration

Sample	The specific surface area <sup>1</sup> SBET, $\text{m}^2 \cdot \text{g}^{-1}$	The pH of the point of zero charge, $\text{pH}_{\text{PZC}}$ <sup>2</sup>	Concentration of carboxyl groups ( $\text{mmol} \cdot \text{g}^{-1}$ )	Concentration of lacton groups ( $\text{mmol} \cdot \text{g}^{-1}$ )	Concentration of phenol groups ( $\text{mmol} \cdot \text{g}^{-1}$ )	Ref.
Pristine xGnP	110	8,5	-	-	-	69
xGnP oxidat cu $\text{HNO}_3$ , la un timp de reflux de o oră	174	2,7	4,5	1,40	1,72	70
xGnP oxidat cu $\text{KMnO}_4$	153	4,3	0,87	1,26	1,09	55
xGnP tratat cu NaOH	135	8,9	0,05	0,03	0,02	58

Sample	The specific surface area <sup>1</sup> SBET, m <sup>2</sup> ·g <sup>-1</sup>	The pH of the point of zero charge, pH <sub>PZC</sub> <sup>2</sup>	Concentration of carboxyl groups (mmol·g <sup>-1</sup> )	Concentration of lacton groups (mmol·g <sup>-1</sup> )	Concentration of phenol groups (mmol·g <sup>-1</sup> )	Ref.
xGnP oxidat cu HNO <sub>3</sub> 65%, la un timp de reflux de 3 ore	208	5,8	5,44	1,25	0,31	63

<sup>1</sup> SBET(Brunauer-Emmet-Teller), m<sup>2</sup>·g<sup>-1</sup>, specific surface area.

<sup>2</sup> pH<sub>PZC</sub>, the pH of the point of zero charge.

Changes in specific surface area (SBET) and pH point of zero charge (pH<sub>PZC</sub>) were consistent with the literature.<sup>56</sup> Specific surface areas were calculated from the adsorption/desorption data using the Brunauer, Emmet, Teller (BET) equations. The specific surface area was measured by nitrogen adsorption-desorption using the BET method at a relative pressure range ( $P/P_0$ ) of 0.0001-0.9900.<sup>57</sup>

Based on the BET equation, the specific surface area was calculated. A higher specific surface area resulted for ox-xGnP obtained by oxidation with 65% HNO<sub>3</sub> with a reflux time of three hours.

The concentration of carboxylic functional groups increased during the three hours of reflux, most likely because these acidic functional groups were progressively formed from the ketone ones. Based on the Boehm titration, which quantifies the concentration of carboxyl groups as a function of different reflux times in the oxidation process using HNO<sub>3</sub>, it appears that their number could be improved up to a certain value of the reflux time of three hours, as can observe in Figure 47. Longer reflux times resulted in a degradative oxidation, possibly based on the localization of acid groups at the edges of the nanoplates layers and their transformation to CO<sub>2</sub> during the longer reflux treatment.

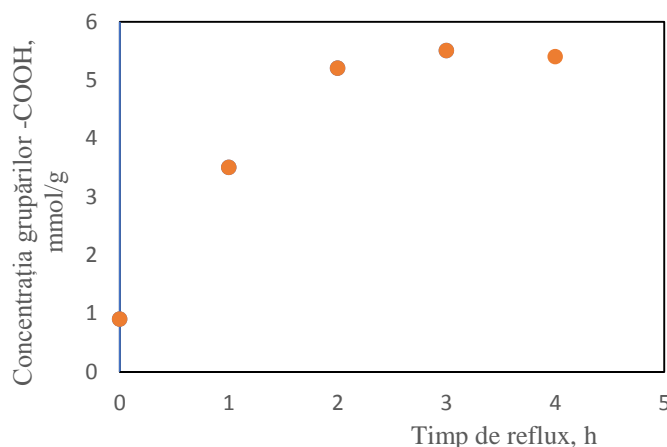


**Figure 47.** The correlation between the calculated concentration of carboxyl groups depending on reflux times (total reflux time is 4 h).

#### 6.5.4. Results and discussion

##### 6.5.4.1. Kinetic studies

The kinetic models used to study the adsorption kinetics on ox-xGnP were pseudo-first-order, pseudo-second-order, and intra-particle diffusion models.<sup>58</sup> In all investigations of the kinetics of the adsorption mechanism, the experimental data were mainly evaluated based on pseudo-first-order (Figure 49) and pseudo-second-order (Figure 51) kinetic models.

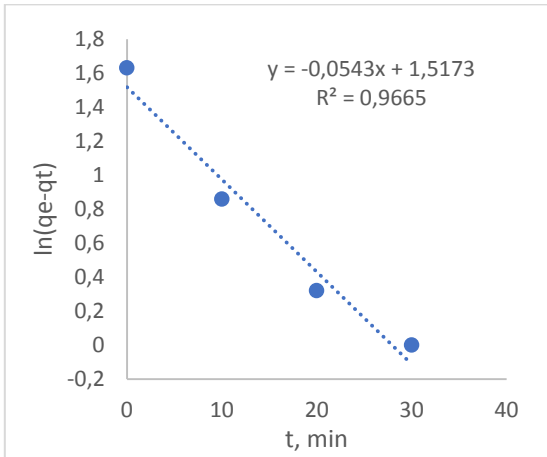


**Figure 49.** Pseudo-first-order kinetic model for ox-xGnP obtained by treatment with HNO<sub>3</sub>, 65%, for three hours, used as sorbent for ammonium ion at 25 °C.

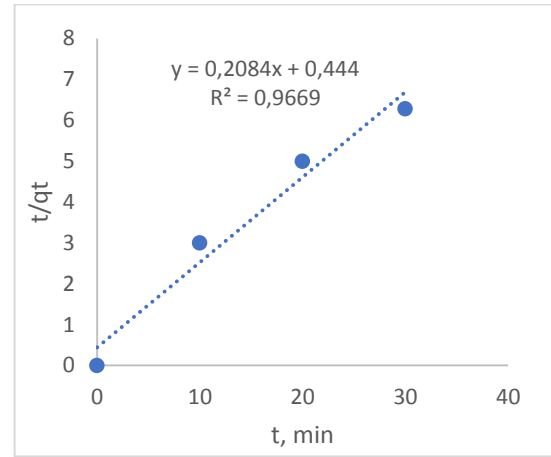


**Figure 50.** Intra-particle diffusion kinetic model for ox-xGnP obtained by treatment with HNO<sub>3</sub>, 65%, for three hours, used as sorbent for the ammonium ions at 25 °C.

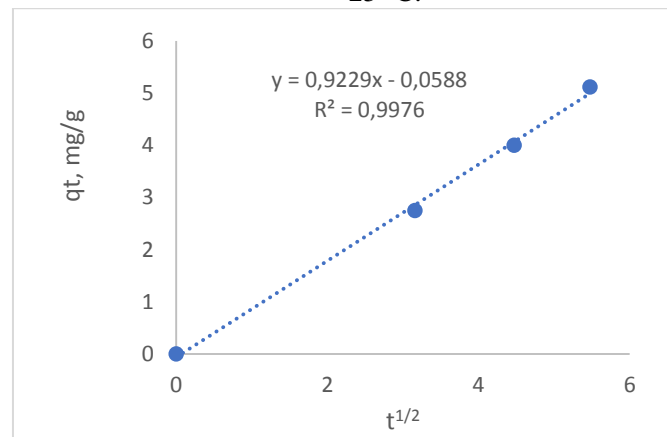


**Figure 51.** The pseudo second-order kinetic model for ox-xGnP obtained by treatment with HNO<sub>3</sub>, 65%, for three hours, used as sorbent for the ammonium ions at 25 °C.

The evaluation of the kinetic models was based on the  $R^2$  value, better values being obtained for the second-order pseudo-kinetic model (Figure 51) and for the intra-particle diffusion model (Figure 50).

It was also observed that the experimental value of the sorption capacity was closer to that calculated by the pseudo-second-order kinetic model, the conclusion being that the sorption process followed this model better, as shown in Table 32. Both chemical and physical interactions play an important role at the ox-xGnP solution-surface interface, while the rate-determining step appears to be determined by diffusion processes: boundary layer diffusion, liquid film diffusion, and internal diffusion, due to the small dimensions of ammonium ions.

**Table 32. Pseudo-first-order and pseudo-second-order kinetic models for removing ions NH<sub>4</sub><sup>+</sup>**

Sorbent (25 °C)	q <sub>e</sub> exp.thesis (mg·g <sup>-1</sup> )	Pseudo-first-order kinetic model			Second-order pseudo-kinetic model			Intra-particle diffusion kinetic model			Ref.
		q <sub>e</sub> cal. (mg·g <sup>-1</sup> )	k <sub>1</sub> (min <sup>-1</sup> )	R <sup>2</sup>	q <sub>e</sub> cal. (mg·g <sup>-1</sup> )	k <sub>2</sub> (g·mg <sup>-1</sup> ·min <sup>-1</sup> )	R <sup>2</sup>	k <sub>id</sub> (mg·g <sup>-1</sup> ·min <sup>-1/2</sup> )	C (mg·g <sup>-1</sup> )	R <sup>2</sup>	
Lignite	3.43	1.31	0.533	0.7080	0.33	5.949	0.999	1.64	1.17	0.9780	<sup>59</sup>
GO	6.6	3.53	0.071	0.9574	6.95	0.037	0.9967				<sup>60</sup>
Ox-xGnP	6.15	1.76	0.049	0.9380	1.47	0.047	0.9560	0.0226	3.01	0.9890	<sup>70</sup>
xGnP	5.65	4.14	0.042	0.9826	2.79	0.001	0.9831				<sup>69</sup>
Ox-xGnP (3h)	6.76	4.43	0.056	0.9238	5.26	0.046	0.9964	0.922	0.58	0.9976	<sup>63</sup>

It can be seen from Table 32 the values of the correlation coefficients that show that the data could be interpreted with other models, for example the double exponential model <sup>61</sup>. Alshameri<sup>62</sup>, considered that a well-fitting pseudo-second-order model involves the movement of ammonium ions to the solid surface, their diffusion from the liquid to the solid surface, and the occurrence of physical and chemical interactions at the surface. Ion exchange is important, possibly being the rate-determining step, but ion exchange processes rely on electrostatic interactions, while acidic functional groups on the surface also involve covalent and ligand bonds.

**6.5.4.2. Study of adsorption isotherms**

Sorption isotherms describe how ammonium ions interact with the ox-xGnP surface, providing information on the type of interactions and their intensity. To describe the effect of these interactions on the adsorption process, the Freundlich and Langmuir models were applied. The Langmuir model relates the adsorption of a monolayer on the homogeneous surface of the adsorbent, based on the linear and non-linear forms below:

$$q_e = \frac{q_m K_L C_e}{1 + K_L C_e}, \tag{47}$$

$$\frac{C_e}{q_e} = \frac{1}{q_m} C_e + \frac{1}{q_m K_L}, \tag{48}$$

An important parameter is the value of R<sub>L</sub>:

$$R_L = 1/(1 + K_L C_0). \tag{49}$$

Equilibrium parameter values for Langmuir R<sub>L</sub> isotherm show unfavorable adsorption (R<sub>L</sub> > 1), favorable adsorption (R<sub>L</sub> < 1), linear adsorption (R<sub>L</sub> = 1) and irreversible adsorption (R<sub>L</sub> < 0).<sup>63</sup>

The Freundlich model is based on multilayer adsorption on the surface of the adsorbent, being an empirical model, where K<sub>F</sub> and n are constants characteristic of this sorption model.

$$\log q_e = \frac{1}{n} \log C_e + \log K_F \tag{50}$$

- where: q<sub>e</sub> – the amount adsorbed at equilibrium (mg·g<sup>-1</sup>),
- q<sub>m</sub> – maximum sorption capacity (monolayer coverage) (mg·g<sup>-1</sup>),
- C<sub>e</sub> – equilibrium concentration (mg·L<sup>-1</sup>),
- K<sub>L</sub> – Langmuir isotherm constant (L·mg<sup>-1</sup>),
- n – the intensity of the adsorption process,

$T$  – temperature (K),

$K_F$  – Freundlich isotherm constant ( $\text{mg}\cdot\text{g}^{-1}$ ),

$R$  – the universal gas constant ( $8,314 \text{ J}\cdot\text{mol}^{-1}\cdot\text{K}^{-1}$ ).

In our case, the Freundlich constant  $n$  represents the intensity of cation exchange, values  $n > 1$  signifying a higher intensity and facilitated chemisorption.<sup>64</sup>

All isotherm experiments were performed at an equilibrium time of three hours, with a solution volume of 50.0 mL, with variations in the initial concentration of  $\text{NH}_4^+$  ions from 20 to 40  $\text{mg}\cdot\text{L}^{-1}$ , at a dose of 10 mg for carbon nanomaterials in all sorption experiments, at three temperatures: 20, 25 and 30 °C, as shown in Figure 52.

Ion exchange processes between ammonium ions and  $\text{H}^+$  ions resulting from the ionization of acid functional groups on the surface are present together with adsorption on hydrophobic sites, determined by intermolecular forces, but ion exchange is also influenced by diffusion processes. It can be seen that the values of  $n$  increase with temperature; consequently, their inverse  $1/n$  values decrease. This aspect proves that it is an exothermic adsorption process, not facilitated by increasing the temperature, based on the values presented in Table 33.

From the comparison of the isotherm parameters, it can be seen, based on the values of the correlation coefficients, that the Langmuir model fits better for the carbon-based nanomaterials used as sorbents for ammonium ions. The sorption process takes place at the surface of the nanomaterial based on hydrophobic interactions and electrostatic interactions and ion exchange in the case of acidic functional groups obtained by oxidation. Regarding the  $q_m$  values, by increasing the number of acidic functional groups on the surface, the values of the maximum adsorption capacity increase, as seen in Figure 53, thus demonstrating that the acidic functional groups on the surface control the ammonium sorption process from aqueous solutions on carbon-based nanomaterials.

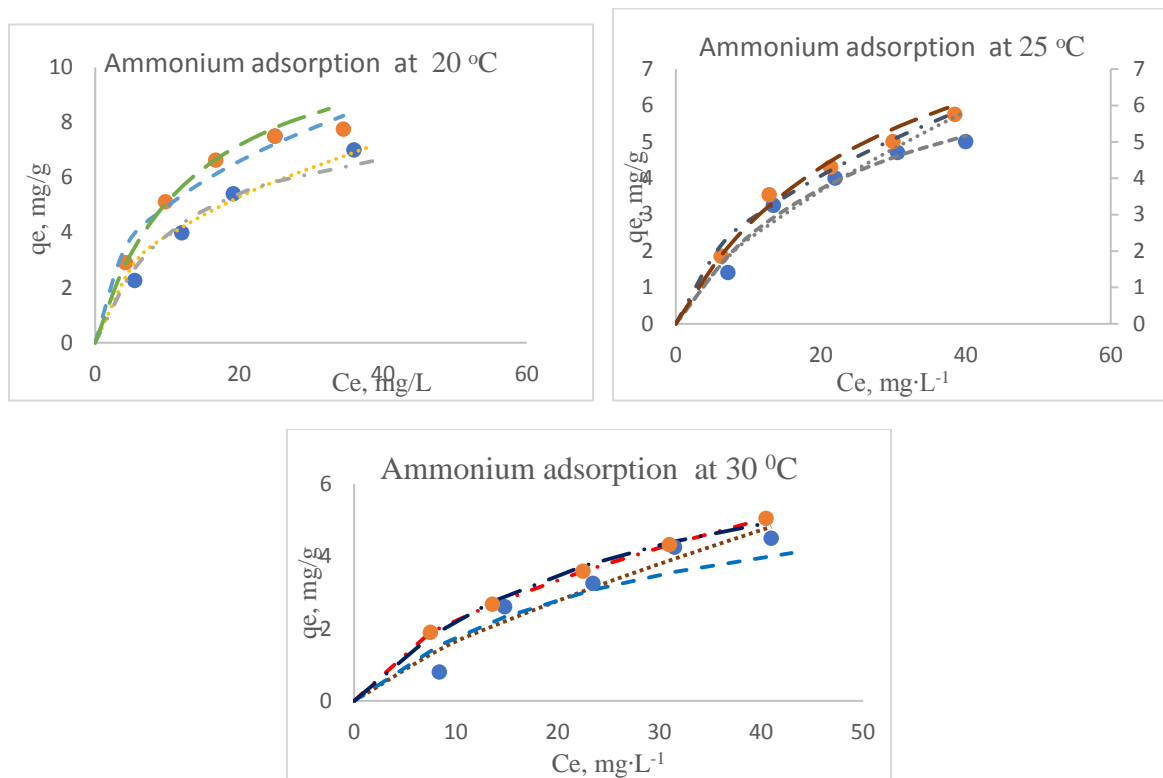


**Figure 52.** Modeling of experimental data obtained in sorption processes for adsorption of ammonium on oxidized xGnP treated with  $\text{HNO}_3$  65%, reflux time of three hours; ... Freundlich model, --- Langmuir model and • experimental data at the three temperatures 20, 25 and 30 °C.

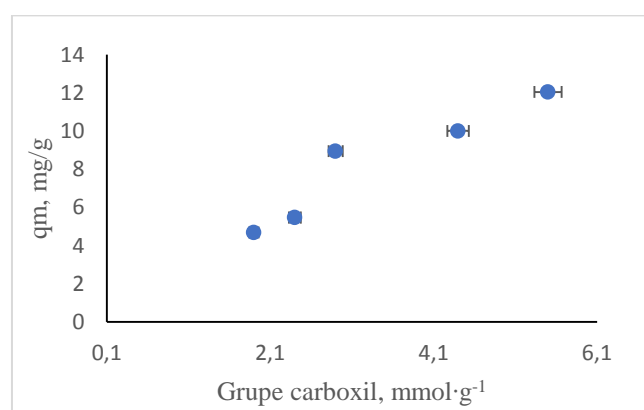
**Table 33.** The values of the parameters of the sorption isotherms for the adsorption of ammonium on ox-xGnP at different temperatures

$T$ (K)	Freundlich				Langmuir			
	Parameter			Performance	Parameter			Performance
	$K_F$	$n$	$1/n$	$R^2$	$K_L$ ( $L \cdot mg^{-1}$ )	$q_m$ ( $mg \cdot g^{-1}$ )	$R_L$	$R^2$
293	1.91	1.45	0.41	0.9851	0.0736	12.04	0.49	0.9922
298	0.79	1.51	0.54	0.9992	0.0346	10.51	0.45	0.9916
303	0.58	1.50	0.58	0.9652	0.0373	8.17	0.42	0.9768

**Table 34.** Parameters of adsorption isotherms based on Freundlich models and Langmuir (non-linear models) for  $NH_4^+$  ions (from the specialized literature)

Sorbent	$T$ °C	Freundlich			Langmuir			Ref.
		$1/n$	$K_F$ , ( $mg \cdot g^{-1}$ )	$R^2$	$q_m$ ( $mg \cdot g^{-1}$ )	$K_L$ ( $L \cdot mg^{-1}$ )	$R^2$	
NaOH Lignite	20	0.43	0.17	0.9570	0.67	0.392	0.997	58
Active charcoal, NaOH	20	2.05	1.81	0.9650	17.03	0.039	0.9800	74
Coconut shell, activated charcoal	25	0.75	0.04	0.9800	5.47	0.003	0.9800	65
AC	20	1.34	0.03	0.9800	5.47	0.003	0.9800	66
ox-xGnP	25	0.39	1.44	0.9649	9.41	0.051	0.9903	57
xGnP	25	1.60	1.06	0.9897	1.66	0.025	0.9987	67
HNO <sub>3</sub> ox-xGnP	25	0.64	0.12	0.9940	10.02	0.079	0.9920	68
NaOH xGnP		0.57	0.58	0.9764	8.17	0.037	0.9743	69
HNO <sub>3</sub> 65%, reflux time 3 h ox-xGnP	20	0.54	0.79	0.9952	12.04	0.034	0.9922	thesis

There have been previous studies showing that the Langmuir and Freundlich models fit better for ammonium adsorption on carbon-based nanomaterials.<sup>70</sup> Our study showed the same: the  $R_L$  values determined for xGnP oxidized with 65% HNO<sub>3</sub>, refluxing the mixture for three hours, were  $<1$ , which means favorable adsorption for ammonium ions under the given experimental conditions, which contribute to the variation of the cluster concentration carboxyl on the surface ox-xGnP. (Figure 53). For the nanomaterials studied, the  $n$  values were greater than 1, with ion exchange processes playing an important role in the ammonium adsorption mechanism.

**Figure 53.** Correlation between the concentration of carboxyl groups on the ox-xGnP surface and the adsorption capacity of carbon-based sorbents.

### 6.5.4.3 Thermodynamic analysis

Thermodynamic analysis provides additional information regarding the internal energy variations of the system during the sorption process. The parameters that can be determined from the value of the thermodynamic distribution coefficient  $K_d$  refer to the changes in the standard Gibbs free energy  $\Delta G^0$  (kJ/mol), the standard enthalpy  $\Delta H^0$  (kJ/mol) and the standard entropy  $\Delta S^0$  (J/mol K).

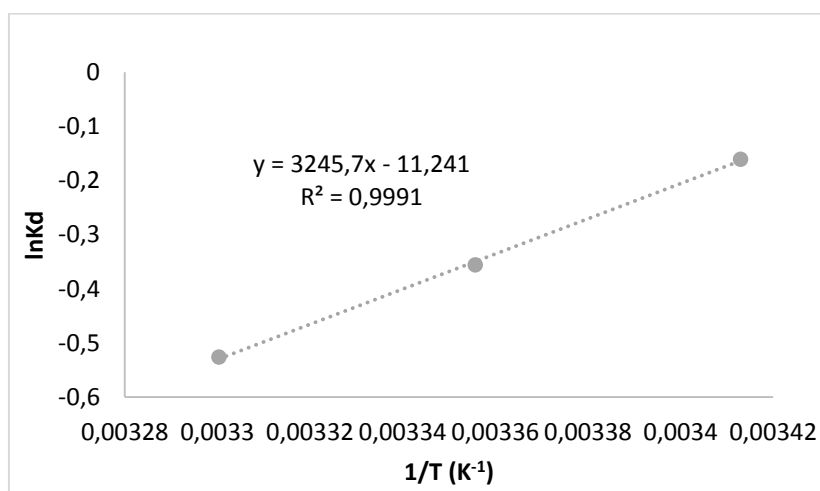


**Figure 54.** The effect of temperature on the ammonium ion sorption process from aqueous solutions on ox-xGnP treated with HNO<sub>3</sub> 65%, reflux time of three hours; T(K): 293, 298 and 303 K; C<sub>i</sub> (ammonium) = 10 mg·L<sup>-1</sup> ; m<sub>sorbent</sub> = 10 mg·L<sup>-1</sup>.

It can be seen from Figure 54 that the sorption capacity decreases with temperature for the studied sorbents, in accordance with the Arrhenius law, if the reaction that takes place on the surface is exothermic, the increase in temperature favoring its development. The values of the thermodynamic parameters obtained from the graphical representation of  $\ln K_d$  vs.  $1/T$  are negative, this indicates a spontaneous, exothermic reaction, ammonium ions being uniformly distributed on the surface of the sorbent at lower temperatures.

### 6.5.4.4. pH influence

From the results obtained in these sorption studies, it was observed that the pH variation in the working aqueous solutions leads to a variation in the value of the maximum sorption capacity for ammonium ions on the oxidized graphite nanoplatelets under the conditions indicated in the experimental part (Figure 55).

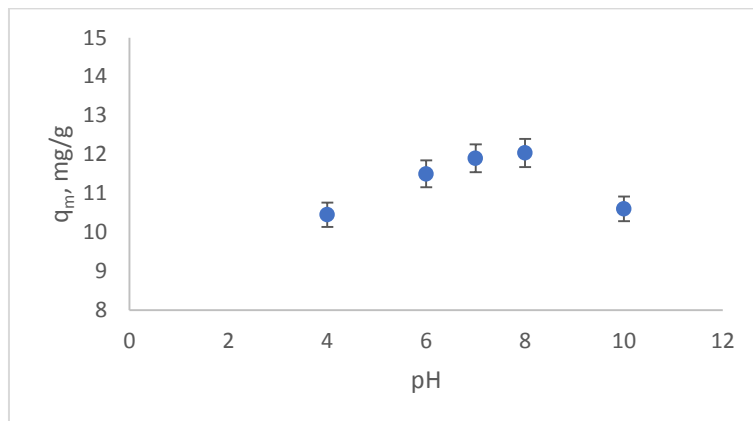


**Figure 55.** The effect of  $pH$  influence on the sorption capacity of nanoplatelets of oxidized graphite for ammonium ions, at a working temperature of 20 °C.

An increase in the sorption capacity for ammonium ions was observed between  $pH$  values between 4 and 7, the sorption capacity then varying very little between  $pH$  values between 7 and 8. This behavior may be due to the presence of functional groups with oxygen introduced by oxidation on the surface of the graphite nanoplatelets and especially of the carboxyl groups  $-\text{COOH}$ . For  $pH$  values between 2 and 7, the carboxyl groups on the surface of the sorbent are protonated, and the electrostatic interactions between the oxidized sorbent surface and ammonium ions are reduced, the sorption process being mainly due to the ion exchange process. As the  $pH$  increases in the range of 7–8, the  $-\text{COOH}$  groups are deprotonated to  $-\text{COO}^-$ , this transformation improving the electrostatic attractions between the ammonium ions and the deprotonated form of the carboxylic groups. For  $pH$  values higher than 8, the sorption capacity of oxidized graphite nanopellets decreases, this may be due to the neutralization reaction of ammonium ions in a weakly basic environment in the presence of  $\text{HO}^-$  ions with ammonia formation, the  $pK_a$  of ammonium having the value 9.24. It can thus be assumed that in the  $pH$  range 7.0–8.0, the carboxyl groups introduced on the surface of graphite nanoplatelets through the oxidation process are deprotonated, and the resulting negatively charged functional groups become electrostatic adsorption centers for ammonium ions.

#### 6.5.4.5. The influence of other cationic species on absorption

The sorption capacity of oxidized graphite nanopellets towards the ammonium ion is also influenced by the presence of other cations in the solution, depending both on their concentration and their valence. Their effect on the sorption capacity was studied, taking into account the average composition of natural waters, choosing monovalent cations such as  $\text{Na}^+$  and  $\text{K}^+$  and bivalent cations such as  $\text{Mg}^{2+}$  and  $\text{Ca}^{2+}$ , with concentration values.

#### 6.5.4.6. Adsorption mechanism

The functional groups that were introduced increased the adsorption capacity, as can be seen in Figure 56. It can be assumed that the number of adsorbed ammonium ions depends on the nature and amount of acid-base functional groups on the surface of the sorbent, on the functional groups of ionic type as well as the  $pH$  of the aqueous solution. These together with the unmodified xGNP surface generate the sorption process through the hydrophobic interactions on the surface of the carbon-based nanomaterial, ion exchange, physisorption and chemisorption processes.

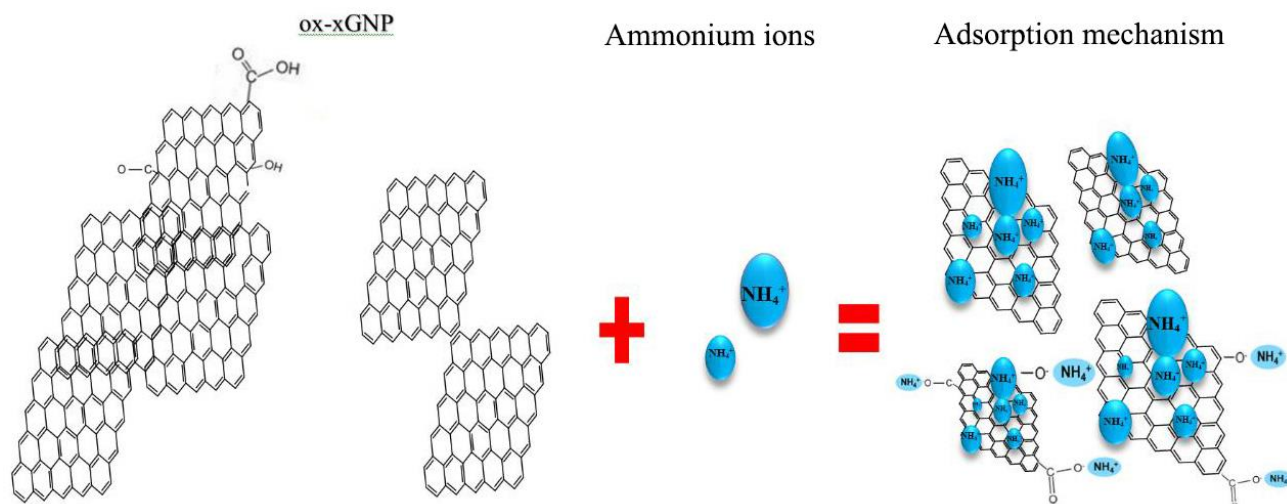


**Figure 57.** Adsorption mechanism of ammonium ions on ox-xGnP.

**Table 37.** The chemical composition of natural water studied before and after ammonium ion sorption on ox-xGnP studied: average values of *pH*, electrical conductivity and average values of concentrations the main ions present in water

Proba	<i>pH</i>	C.e. $\mu\text{S}\cdot\text{cm}^{-1}$	$\text{Cl}^{-}$ $\text{mg}\cdot\text{L}^{-1}$	$\text{SO}_4^{2-}$ $\text{mg}\cdot\text{L}^{-1}$	$\text{HCO}_3^{-}$ $\text{mg}\cdot\text{L}^{-1}$	$\text{F}^{-}$ $\text{mg}\cdot\text{L}^{-1}$	$\text{NH}_4^{+}$ $\text{mg}\cdot\text{L}^{-1}$	$\text{NO}_3^{-}$ $\text{mg}\cdot\text{L}^{-1}$
S1 initial	6.6	1517	10.28	20.65	1189	0.41	0.06	0.072
S1 final	6.09	1500	9.3	18.7	-	0.3	0.014	0.07
S2 initial	6.12	1247	1.61	9.11	1130	0.31	0.088	0.037
S2 final	6.04	1220	1.5	8.0	-	0.23	0.056	0.029
S3 initial	5.98	1449	1.03	2.68	960	0.25	0.05	0.046
S3 final	5.87	1428	0.84	2.20	-	0.11	0.023	0.039

The results obtained after the treatment of some natural water samples with studied ox-xGnP-based sorbents lead to the conclusion that they can be used for the removal of ammonium ions with reduced concentrations of cations and higher concentrations of anions, as shown in Table 37. Concentrations of hydrogencarbonate ions were determined only in the initial samples, because in the final samples, the values of *pH* and electrical conductivities did not vary significantly.

Removal of ammonium ions from natural waters using oxidized carbon nanoplatelets (ox-xGnP) by refluxing for three hours with 65%  $\text{HNO}_3$ . Ox-xGnP proved to be a good adsorbent for ammonium ions, depending on the type and concentration of oxygen-containing functional groups on the carbon surface.

## Chapter 7. Final conclusions

The thesis "Carbon-based nanomaterials in the treatment of natural waters" presents in the theoretical part a classification of natural waters and their treatment methods, emphasizing the sorption methods used for this purpose, using carbon-based nanomaterials as sorbents.

The chemical and radiochemical species that enter the composition of natural mineral waters were determined, and from the analysis of their radiochemical composition, small variations of the composition were observed depending on the season, falling within a maximum margin of 10%.

Variations in the concentrations of radionuclides  $^{40}\text{K}$ ,  $^{238}\text{U}$ ,  $^{232}\text{Th}$  and  $^{226}\text{Ra}$  in the studied mineral waters indicate that, although the origins of these water samples are the same, they come from different depths and pass through different geological layers. Through radiometric spectrometry methods, the content of radionuclides in mineral waters was determined, as well as their radioactivity, obtaining new data sets. The average annual effective doses for all analyzed water samples are between 15.45–47.38  $\mu\text{Sv}\cdot\text{year}^{-1}$ , all of which are well below the reference level of the effectively admitted dose (100  $\mu\text{Sv}\cdot\text{year}^{-1}$ ) recommended by the WHO and they comply with Directive 2009/54/EC of the European Parliament.

Methods for the analysis of nitrate, nitrite and ammonium ions were developed, through chromatographic methods for the separation of cationic and anionic species, improvements were observed due to the prior degassing of the samples subjected to analysis and the use of separation columns of different lengths, in order to obtaining an increased selectivity.

This study revealed an influence of the distribution of nitrate, nitrite and ammonium ions following the sanitization treatment of natural mineral water bottling facilities, using oxygenated water as a sanitizing agent for collecting tanks. Several factors have been studied that influence the types of nitrogen compounds that appear and the variation in their distribution.

The oxidation of  $\text{NH}_4^+$  ions finally leads to a decrease in their initial concentration, the nitrate concentration increasing due to the oxidation of ammonium ions, in direct correlation with both the initial ammonium concentration and the initial nitrogen concentration in the matrix.

The *pH* values increase after using  $\text{H}_2\text{O}_2$  as a sanitizing agent, but considering the slightly acidic initial *pH* value in carbonated mineral waters, this increase does not affect either the taste or the chemical composition of most compounds.

Studies were made on the sorption of ammonium ions from synthetic aqueous solutions using oxidized carbon nanoplatelets (ox-xGnP) as sorbents through different procedures. Oxidized carbon nanoplatelets (ox-xGnP) show a better sorption capacity for ammonium ions compared to xGnP. The adsorption characteristics were examined at different contact times, at different initial concentrations of ammonium ions, *pH* values and temperatures, respectively. The experimental results of the sorption studies for ammonium ions in aqueous solutions were interpreted based on the Langmuir, Freundlich, Temkin and Harkins-Jura models. Kinetic studies are based on the pseudo-first-order kinetic model of a Lagergreen curve, the pseudo-second-order model, and the intra-particle diffusion model to elucidate the adsorption mechanisms and controlled adsorption rates. The temperature dependence of ammonium ion adsorption was also studied and thermodynamic parameters  $\Delta H^\circ$ ,  $\Delta G^\circ$  and  $\Delta S^\circ$  were calculated, resulting in data that described the exothermic process.

Adsorption mechanisms include chemical and physical interactions, ammonium adsorption on ox-xGnP being based on ion exchange, chemisorption and physical adsorption processes. Based on its chemical and structural stability, ox-xGnP could become a good sorbent applied in natural water treatment.

The ox-xGnP sorbents present a multifunctional character that could be exploited for the simultaneous removal of several species present in natural waters, both chemical and radiochemical. Beyond these applications, the assembly of ox-xGnP into macroscopic hybrid architectures with controllable pore sizes could significantly improve the sorption capacities of the new sorbents for inorganic, organic, and microbiological contaminants.

When choosing the methods of treating natural and mineral waters, the methods allowed by legislation must be taken into account. Taking into account that graphite nanoplatelets can represent a substitute for activated carbon in the treatment processes of these types of water, their advantages are given by the much reduced amount in which they can be used. Oxidized xGnP, with different degrees of oxidation, using different oxidizing agents, show increased selectivity compared to activated carbon towards certain chemical species. The regeneration of these sorbents is also possible, and the reduced degree of toxicity of these carbon-based nanostructures makes it possible to use them in various industrial applications

## List of published works and participation in conferences

### List of published papers:

Ion, I.; **Bogdan, D.**; Ion, A.C. Improvement in the determination of traces of nitrate and nitrite in natural mineral waters by ion chromatography. *UPB Sci. Bull. Ser. B. Chem. Mater. Sci.*, **2014**, 76, 113–122.

**Bogdan, D.**; Rizea, G.A.; Ion, I.; Ion, A.C.; Ammonium adsorption on exfoliated graphite nanoplatelets. *Rev. Chim.*, **2016**, 67, 2231–2236, **IF = 1.755**, WOS:000388361900022

M.R. Călin, I. Rădulescu, I. Ion, **D. Bogdan**, A. C. Ion - Radiometric Studies on Carbonated Natural Mineral Waters from the Northern Part of Romania, *Rev. Chim.*, **2016**, 67, 2537–2540, **IF = 1.755**, WOS:000393230400031

**Bogdan, D.**; Muklive, A.J.S.; Ion, I.; Ion, A.C. Ammonium adsorption on oxidized exfoliated graphite nanoplatelets, *Environ. Eng. Manag. J.*, **2017**, 16, 543–552, **IF = 0.858**, WOS:000403508600005

**Bogdan D.**, Ion I., Sirbu F., Ion A. C. - A possible distribution of nitrogen compounds during natural mineral waters disinfection treatment, *Environ. Eng. Manag. J.*, **2017**, 16, 597-603, **IF = 0.858**, WOS:000403508600011

Ion I., Ion A. C., Călin M. R., Rădulescu I., **Bogdan, D.** - Assessment of chemical parameters and natural radionuclides concentrations in carbonated natural mineral water and contribution to radiation dose I, *Romanian Journal of Physics*, **2019**, 64 (804), 1-14, **IF = 1.662**, WOS:000460671400013

Ion I., **Bogdan, D.**, Mincu, M. M., Ion, A. C. - Modified Exfoliated Carbon Nanoplatelets as Sorbents for Ammonium from Natural Mineral Waters Ion, *Molecules*, **2021**, 26 (3541), 2-15, **IF=4.927**, WOS:000666059400001

Total IF=1,755+1,755+0,858+0,858+1,662+4.927= 11,815

### Papers presented at conferences:

**Daniela Bogdan**, Al-Ogaidi Ahmed Jassim Muklive, Ion Ion, Alina Catrinel Ion, Ammonium adsorption on exfoliated graphite nanoplatelets , 8<sup>th</sup> International conference on environmental engineering and management 9-12 September 2015, Iasi Romania, S1.3, p13

**Daniela Bogdan**, Ion Ion, Alina Catrinel Ion, Possible distribution the nitrogen compounds during natural mineral water disinfection treatment, 8<sup>th</sup> International conference on environmental engineering and management 9-12 September 2015, Iasi Romania, S6-P6, p27

**Daniela Bogdan**, Al-Ogaidi Ahmed Jassim Muklive, Ion Ion, Alina Catrinel Ion - Ammonium removal from aqueous solutions using oxidized graphite based Nanomaterials, University Politehnica of Bucharest, Department of Analytical Chemistry and Environmental Engineering, Environmental Engineering, Polizu Street no. 1-7, 011061, Bucharest, Romania, SEVENTEENTH ANNUAL CONFERENCE YUCOMAT 2015, Herceg Novi, August 31-September 4, 2015, P.S.C.10, p. xxxii

## REFERENCES (Selective bibliography)

- 1 European Union (2005), List of natural mineral waters recognized by member states. Off. J. Eur. Communities 7-32 EEA 2005/C 59/06
- 2 EU Directive 1980/778/EEC, 1980a Council directive 1980/778/EEC on the approximation of the laws of the Member States relating to the exploitation and marketing of natural mineral water Off. J. Eur. Communities L229, 1-10 30.08.1980
- 3 EU Directive 1996/70/EC of the European Parliament and of the Council of 28 October 1996 amending Council Directive 80/777/EC on the approximation of the laws of the Member States relating to the exploitation and marketing of natural mineral waters. Off. J. Eur. Communities L299, 26-28 23.11.1996
- 4 EU Directive 2003/40/EC, 2003 Establishing the list, concentration limits and labeling requirements for the constituents of natural mineral waters and the conditions of using ozone-enriched air for the treatment of natural mineral waters and spring waters. Off. J. Eur. Communities L 126, 34-39 22.05.2003
- 5 IUPAC, *Compendium of chemical terminology, The gold book*, 2nd ed. Blackwell Science, Oxford, UK, **1997**, <http://old.iupac.org/publications/books/author/mcnaught.html>
- 6 Ion A.C.; Ion I.; Antonisse M.M.; Snellink-Ruel B.H.M.; Reinhoudt D.N., Characteristics of fluoride-selective electrode with uranyl salophen receptors in aqueous solutions, *Russ. J. General Chem.*, **2001**, 71(2), 159-161.
- 7 Banks D.; Frengstad B.; Midgard A.K.; Krog, J.R.; Strand T. The chemistry of Norwegian groundwaters: I. The distribution of radon, major and minor elements in 1604 crystalline bedrock groundwaters. *Sci. Total Environ.*, **1998**, 222, 71-91.
- 8 Bellia, C.; Gallardo A.H.; Yasuhara M.; Geochemical characterization of groundwater in volcanic system, *Resources*, **2015**, 4, 358-377.
- 9 Scheiber L.; Ayora, C.; Vasquez-Sune E.; Cendon D.I.; Soler A.; Baquero, J.C. Origin of high ammonium, arsenic and boron concentrations in the proximity of a mine. Natural vs. anthropogenic processes, *Sci. Total Environ.*, **2016**, 541, 655-666.
- 10 Bucur A. *Elemente de chimia apei*, Ed. H\*G\*A\*, București, **1999**.
- 11 Caschetto M.; Winner A. Ammonium natural attenuation in complex hydrogeological settings: insights from a multi-isotope approach, *Italian J. Groundwater*, **2017**, As23-307, 7-13.
- 12 Pintilie V.; Ene A.; Georgescu L.P.; Moraru D.I. Gross alpha, gross beta and <sup>40</sup>K activities and daily effective dose due to natural radionuclides from food supplements, *Rom. J. Pys.*, **2017**, 62, 703
- 13 Tannenbaum S.R.; Walstra, P. *Handbook of Water Analysis*, Edit. Nollet L.M., M. Dekker, New York, **2000**.
- 14 Kim, J-H.; LEE J-H. Simultaneous Determination of Six Cations in Mineral Water by Single-column Ion Chromatography. *J. Chromatogr.*, **1997**, 782, 140-146.
- 15 Schumann, H.; ERNST M. Monitoring of Ionic Concentrations in Airborne Particles and Rain Water in an Urban Area of Central Germany. *J. Chromatogr.*, **1993**, 640, 241-249.

- 
- 16 Rocklin, R. D.; Rey, M. A.; Stillian, J. R.; Campbell, D. L. Ion Chromatography of Monovalent and Divalent Cations. *J. Chromatogr. Sci.*, **1989**, *27*, 474-482.
- 17 Hoffman, P.; Karandashev V. K.; Sinner T.; Ortner H. M. Chemical Analysis of rain and Snow Samples from Chernogolovka/Russia by, IC, TXRF and ICP-MS. *Fresenius J. Anal. Chem.*, **1997**, *357*, 1142-1148.
- 18 Jackson, P. E. Determination of Inorganic Ions in Drinking Water by Ion Chromatography. *Trends Anal. Chem.*, **2001**, *20*, 320-329.
- 19 Astel A.; Mazerski, J.; Polkowska Z.; Namiesnik, J. Application of PCA and Time Series Analysis in Studies of Precipitation in Tricity (Poland). *Advan. Environ. Res.*, **2004**, *8*, 337-349.
- 20 Gibb S.; Mantoura R. Fauzi, C.; Liss, P. S. Analysis of Ammonia and Methylamines in Natural Waters by Flow Injection Gas Diffusion Coupled to Ion Chromatography. *Anal. Chim. Acta.*, **1995**, *316*, 291-304.
- 21 EN ISO 2009. Water Quality. Determination of dissolved anions by liquid chromatography of ions. Determination of fluoride, chloride, nitrite, orthophosphate, bromide, nitrate and sulfate ions. Method for water with low contamination EN ISO 10304-1. European Committee for standardization/International Organization for Standardization, Brussels, Belgium/Geneve, Switzerland, **2009**.
- 22 Pulgarin, C.; Fe vs. TiO<sub>2</sub> photo-assisted processes for enhancing the solar inactivation of bacteria in water, *Chimia*, **2015**, 7-9.
- 23 Nidhees, P.; Gandhimathi R.; Ramesh S. Degradation of dyes form aqueous solutions by Fenton processes: a review, *Environmental Science and Pollution Research*, **2013**, *20*, 2099-2132.
- 24 Chidambara, C.B.; Quen H.L. Advanced oxidation process for wastewater treatment: optimization of UV/H<sub>2</sub>O<sub>2</sub> process through a statistical technique, *Chemical Engineering Science*, **2005**, *60*, 5305-5311.
- 25 Malato S.; Fernández-Ibáñez, P.; Maldonado M.I.; Blanco, J.; Gernjak, W. Decontamination and disinfection of water by solar photocatalysis: Recent overview and trends, *Catalysis Today*, **2009**, *147*, 1-59.
- 26 Pulgarin, C.; Kiwi, J. Overview on photocatalytic and electrocatalytic pretreatment of industrial non-biodegradable pollutants and pesticides, *Chimia*, **1996**, *50*, 50-55.
- 27 Ryu, H., Thompson, D., Huang, Y., Li, B., Lei, Y., Electrochemical sensors for nitrogen species: a review, *Sensors and Actuators Reports*, **2020**, *2*(1), 100022.
- 28 EU Directive 54, (2009), EU Directive 2009/54/EC of the European Parliament and of the Council, June 18<sup>th</sup> 2009, on the exploitation and marketing of natural mineral waters, Official Journal of the European Union, **L164**, 45-58.
- 29 Kavitha V.; Palanivelu K. The role of ferrous ion in Fenton and photo-Fenton processes for the degradation of phenol, *Chemosphere*, **2004**, *55*, 1235-1243.
- 30 Nidhees, P.; Gandhimathi R.; Ramesh S. Degradation of dyes form aqueous solutions by Fenton processes: a review, *Environmental Science and Pollution Research*, **2013**, *20*, 2099-2132.
- 31 Kotzias D.; Hustert K.; Wieser A. Formation of oxygen species and their reactions with organic chemicals in aqueous solution, *Chemosphere*, **1987**, *55*, 1235-1243.
- Kotzias D.; Hustert K.; Wieser A. Formation of oxygen species and their reactions with organic chemicals in aqueous solution, *Chemosphere*, **1987**, *16*, 505-511.

- 
- 32 Kotzias D.; Hustert K.; Wieser A. Formation of oxygen species and their reactions with organic chemicals in aqueous solution, *Chemosphere*, **1987**, *55*, 1235-1243.
- Kotzias D.; Hustert K.; Wieser A. Formation of oxygen species and their reactions with organic chemicals in aqueous solution, *Chemosphere*, **1987**, *16*, 505-511.
- 33 Toriyama, K.; Fukae, K.; Suda, Y.; Tomofumi Kiyose; Takumi Oda; Fujii, Y.; Nguyen Doan Thien Chi; Duong Huu Huy; To Thi Hien; Takenaka, N. NO<sub>2</sub> and HONO concentrations measured with filter pack sampling and high HONO/NO<sub>2</sub> ratio in Ho Chi Minh city, Vietnam, *Atmospheric Environ.*, **2019**, 116865 (1-7).
- 34 Qu, X.; Alvarez, P.J.J.; Li Q. Applications of nanotechnology in water and wastewater treatment, *Water Res.*, **2013**, *47*, 3931–3946.
- 35 Upadhyayayula V.K.K.; Deng S.; Mitchell M.C.; Smith G.B. Application of carbon nanotube technology for removal of contaminants in drinking water: a review, *Sci. Total Environ.*, **2009**, *408*, 1–13.
- 36 Qu, X.; Alvarez, P.J.J.; Li Q. Applications of nanotechnology in water and wastewater treatment, *Water Res.*, **2013**, *47*, 3931–3946.
- 37 Tang, Y.; Alam, M.S.; Konhauser, K.O.; Alessi, D.S.; Xu, S.; Tian, W.; Liu, Y. Influence of the pyrolysis temperature on production digested sludge biochar and its application for ammonium removal from municipal wastewater. *J. Clean. Prod.*, **2019**, *209*, 927–936.
- 38 Seredych, M.; Bandoz , T. J.; Mechanism of ammonia retention on graphite oxides: role of surface chemistry and structure, *J. Phys. Chem. C*, **2007**, *111*, 15596–15604.
- 39 Petit, C.; Seredych M.; Bandoz T.J. Revisiting the chemistry of graphite oxides and its effect on ammonia adsorption, *J. Mater. Chem.*, **2009**, *19*, 9176–9185.
- 40 Goncalves M.; Sanchez-Garcia L.; Oliveira Jardim E.D.; Silvestre-Albero, J.; Rodriguea-Reinoso F. Ammonia removal using activated carbons: effect of the surface chemistry in dry and moist conditions, *Environ. Sci. Technol.*, **2011**, *45*, 10605–10610.
- 41 Feng, W.; Kwon S.; Bourguet E.; Vidic R. Adsorption of hydrogen sulfide onto activated carbon fibers: effect of pore structure and surface chemistry, *Environ. Sci. Technol.*, **2005**, *39*, 9744–9749.
- 42 Kang, S.; Pinault, M.; Pfefferle, L. D.; Elimelech, M.; Single-Walled Carbon Nanotubes Exhibit Strong Antimicrobial Activity, *Langmuir*, *23*, 8670–8673.
- Kim K.-J.; Ahn H.-G. The effect of pore structure of zeolite on the adsorption of VOCs and desorption properties by microwave heating, *Microporous Mater.*, **2012**, *152*, 78–83.
- 43 Seredych M.; Bandoz T.J. Mechanism of ammonia retention on graphite oxides: role of surface chemistry and structure, *J. Phys. Chem., C*, **2007**, *111*, 15596–15604.
- 44 Seredych M.; Bandoz T.J. Removal of ammonia by graphite oxide via its intercalation and reactive adsorption, *Carbon*, **2007**, *45*, 2130–2132.
- 45 Seredych M.; Rossin, J.A.; Bandoz T.J. Changes in graphite oxide texture and chemistry upon oxidation and reduction and their effect on adsorption of ammonia, *Carbon*, **2011**, *49*, 4392–4402.
- 46 Tang S.; Cao Z. Adsorption and dissociation of ammonia on graphene oxides: a first-principles study, *J. Phys. Chem., C.*, **2012**, *116*, 8778–8791.

- 
- 47 Sabsehmeidani, M.M., Mahnaee, S., Ghaedi, M., Heidari, H., Roy, V.A.L., Carbon based materials: A review of adsorbents for inorganic and organic compounds, *Mater. Adv.*, **2021**, 2, 598-627.
- 48 De la Luz-Assuncion, M., Sanchez-Mendieta, V., Martinez-Hernandez, A.L., Castano, V.M., Velasco-Santos, C., Adsorption of phenol from aqueous solutions by carbon nanomaterials of one and two dimensions: kinetic and equilibrium studies, *J. Nanomaterials*, **2015**, 176, 405036.
- 49 Mohan D.; Pittman, C.U. Jr. Activated carbons and low cost adsorbents for remediation of tri- and hexavalent chromium from water, *J. Hazard. Mater.*, **2006**, 137, 762–811.
- 50 Upadhyayayula V.K.K.; Deng S.; Mitchell M.C.; Smith G.B. Application of carbon nanotube technology for removal of contaminants in drinking water: a review, *Sci. Total Environ.*, **2009**, 408, 1–13.
- 51 Wang, X. et al. Synthesis of novel nanomaterials and their applications in efficient removal of radionuclides *Science China Chemistry*, **2019**, 62(8), 933-967.
- 52 Gonçalves, M.; Sánchez-García, L.; de Oliveira Jardim, E.; Silvestre-Albero, J.; Rodríguez-Reinoso, F.; Ammonia Removal Using Activated Carbons: Effect of the Surface Chemistry in Dry and Moist Conditions, *Environ. Sci. Technol.*, **2011**, 45, 10605–10610.
- 53 Gonzales-Guerrero, A.B.; Mendoza, E.; Pellicer, E.; Alsina, F.; Fernandez-Sanchez, C.; Lechuga, L.M. Discriminating the carboxylic groups from the total acidic sites in oxidized multi-wall carbon nanotubes by means of acid-base titration. *Chem. Phys. Lett.*, **2008**, 462, 256–259.
- 54 Spataru, P. Influence of organic ammonium derivatives on the equilibria between ammonium, nitrite and nitrate ions in the Nistru river water. *Scientific Reports*, **2022**, 12, 13505.
- 55 Ion, A.C.; Ion, I.; Culetu, A. Lead adsorption onto exfoliated graphitic nanoplatelets in aqueous solutions. *Mater. Sci. Eng. B.*, **2011**, 176, 504–509.
- 56 Gusain, R.; Kumar, N.; Ray, S.S. Recent advances in carbon-nanomaterial-based adsorbents for water purification. *Coord. Chem. Rev.*, **2020**, 405, 213111.
- 57 Quach, N.K.N.; Yang, W.D.; Chung, Z.J.; Tran, H.L. The influence of the activation temperature on the structural properties of the activated carbon xerogels and their electrochemical performance. *Ann. Mater. Sci. Eng.*, **2017**, 9, 1-10.
- 58 Kizito, S.; Wu, S.; Kirui, W.K.; Lei, M.; Lu, Q.; Bah, H.; Dong, R. Evaluation of slow pyrolyzed wood and rice husks biochar for adsorption of ammonium nitrogen from piggery manure and anaerobic digestate slurry. *Sci. Total Environ.*, **2015**, 505, 102–112.
- 59 Tu, Y.N.; Feng, P.; Ren, Y.G.; Cao, Z.H.; Wang, R.; Xu, Z.Q. Adsorption of ammonia nitrogen on lignite and its influence on coal water slurry preparation. *Fuel*, **2019**, 238, 34–43.
- 60 Wu, C.; Zhang, X.; Li, C.; Cheng, C.; Zheng, Y. Adsorption of ammonium by graphene oxide based composites prepared by UV irradiation and using a slow-release fertilizer, *J. Polym. Environ.*, **2018**, 26, 4311–4320.
- 61 Ion, I., Bogdan, D., Mincu, M.M., Ion, A.C., Modified exfoliated carbon nanoplatelets as sorbents for ammonium from natural mineral waters, *Molecules.*, **2021**, 26(12), 3541.

- 
- 62 Alshameri, A.; He, H.P.; Zhu, J.X.; Xi, Y.F.; Zhu, R.L.; Ma, L.Y.; Tan, Q. Adsorption of ammonium by different natural clay minerals: Characterization, kinetics and adsorption isotherms. *Appl. Clay Sci.*, **2018**, *159*, 83–93.
- 63 Reguyal, F.; Sarmah, A.K.; Gao, W. Synthesis of magnetic biochar from pine sawdust via oxidative hydrolysis of FeCl<sub>2</sub> for the removal sulfamethoxazole from aqueous solution, *J. Haz. Mater.*, **2017**, *321*, 868–878.
- 64 Foo, K. Y.; Hammed, B.H. Insights into the modelling of adsorption isotherm systems, *Chem. Eng. J.*, **2018**, *158*, 2–20.
- 65 Rambabu, N.; Rao, B.V.S.K.; Surisetty, V.R.; Das, U.; Dalai, A.K. Production, characterization and evaluation of activated carbon from de-oiled canola meal for environmental applications, *Ind. Crop. Prod.*, **2015**, *65*, 572–581.
- 66 Sumaraj, X.; Sarmah, A.K.; Padhye, L.P. Acidic surface functional groups control chemisorption of ammonium onto carbon materials in aqueous media, *Sci. Total. Env.*, **2020**, *698*, 134193.
- 67 Bogdan, D.; Rizea, G.A.; Ion, I.; Ion, A.C.; Ammonium adsorption on exfoliated graphite nanoplatelets. *Rev. Chim.*, **2016**, *67*, 2231–2236.
- 68 Bogdan, D.; Muklive, A.J.S.; Ion, I.; Ion, A.C. Ammonium adsorption on oxidized exfoliated graphite nanoplatelets, *Environ. Eng. Manag. J.*, **2017**, *16*, 543–552.
- 69 Mathurasa, S.; Damrongsiri S. Low cost and easy rice husk modification to efficiently enhance ammonium and nitrate adsorption. *Intern. J. Recyc. Org. Waste Agric.*, **2018**, *7*, 143–151.
- 70 Gai, X.; Wang, H.; Liu, J.; Zhai, L.; Liu, S.; T.; Ren, T. Effects of feedstock and pyrolysis temperature on biochar adsorption of ammonium and nitrate. *PLoS ONE*, **2014**, *9*, 1–19.